Plant viruses transmitted in two different modes produce differing effects on small RNA-mediated processes in their aphid vector

Patricia V. Pinheiro,[a,b,c,] Jennifer R. Wilson,[b,d] Yi Xu[d], Yi Zheng,[b] Ana Rita Rebelo,[b] Somayeh Fattah-Hosseini,[b] Angela Kruse,[b,d] Rogerio Santos Dos Silva,[b] Yimin Xu,[b] Matthew Kramer[e], James Giovannoni,[b,f,g] Zhangjun Fei,[b,d] Stewart Gray,[d,h] and Michelle (Cilia) Heck[b,d,h,#]

Department of Entomology, Cornell University, Ithaca, New York, USA[a]; Boyce Thompson Institute for Plant Research, Ithaca, New York, USA[b]; Embrapa Rice and Beans, Santo Antônio de Goiás, Brazil[c]; Section of Plant Pathology and Plant-Microbe Biology, School of Integrated Plant Science, Cornell University, Ithaca, New York, USA[d]; USDA Agricultural Research Service, Statistics Group, Beltsville, Maryland, USA[e]; USDA Agricultural Research Service, Plant, Soil and Nutrition Research Unit, Ithaca, New York, USA[f]; Section of Plant Biology, School of Integrated Plant Science, Cornell University, Ithaca, New York[g]; USDA Agricultural Research Service, Emerging Pest and Pathogen Research Unit, Ithaca, New York, USA[h]

Address correspondence to Michelle Heck, michelle.cilia@ars.usda.gov, mlc68@cornell.edu

P.V.P. and J.R.W contributed equally to this work.

22 **ABSTRACT**

23 Transmission of plant viruses by aphids involves multi-trophic interactions among host
24 plants, aphid vectors, and plant viruses. Here, we used small RNA (sRNA) sequencing
25 to visualize the sRNA response of *Myzus persicae* to two plant viruses that *M. persicae*
26 transmits in different modes: the nonpersistent *Potato virus Y* (PVY) versus the
27 persistent *Potato leafroll virus* (PLRV). Aphids exposed to PLRV produced significantly
28 less 22mers aligned to the aphid genome, and an abundance of 26-27mers, many of
29 which were predicted to be piRNA. Additionally, expression of *Buchnera aphidicola*
30 tRNA-derived sRNAs was influenced by PLRV and, to a lesser extent, PVY, suggesting
31 that plant viruses alter the aphid-endosymbiont relationship. Finally, aphids exposed to
32 PLRV-infected plants generated an abundance of unusually long sRNAs and a reduced
33 number of 22mers against an aphid virus, *Myzus persicae densovirus* (MpDNV) and
34 had higher MpDNV titer. Expression of the PLRV silencing suppressor P0 in plants
35 recapitulated the increase in MpDNV titer in the absence of PLRV infection. Our results
36 show that plant viruses transmitted in two different modes cause distinct effects on their
37 vector with regards to post-transcriptional gene regulation, symbiosis with *Buchnera,*
38 and the antiviral immune response of aphids to an aphid-infecting densovirus.

INTRODUCTION

Aphids are the most important and widespread vectors of plant viruses (Nault, 1997, Ng & Falk, 2006). Together, aphids and the plant viruses they transmit cause significant crop yield losses around the world. Transmission of plant viruses by aphids involves co-evolved, multi-trophic interactions among the plant host, the aphid vector, and the plant virus. In the molecular tug-of-war of plant virus infection and transmission, plant hosts activate their immune defenses against aphids and plant viruses, and the latter two use a myriad of strategies to overcome the host plant defenses. For instance, plant viruses encode silencing suppressor proteins to impair the plant antiviral immune system (Ding & Voinnet, 2007, Li & Ding, 2006, Mlotshwa et al., 2008).

Aphid-borne plant viruses are transmitted by their aphid vectors via distinct modes of transmission, such as nonpersistent, stylet-borne or persistent circulative (Nault, 1997). For instance, the green peach aphid, *Myzus persicae,* can transmit over 100 different plant viruses, including the persistent, circulative *Potato leafroll virus* (PLRV) and the nonpersistent *Potato Virus Y* (PVY), which both infect plants in the Solanacea family (Kennedy et al., 1962). Nonpersistent viruses do not circulate through the insect vector tissues when transmitted. Upon ingestion, nonpersistent viruses stay bound to the aphid stylet for a short period where they can be transmitted to a new host plant upon probing. On the other hand, persistently transmitted viruses, such as the plant viruses in the family *Luteoviridae*, referred to as luteovirids hereafter in this paper, circulate through the insect vector tissues to be transmitted to a new host plant (for a review, see (Gray et al., 2014)). Luteovirids are transmitted exclusively by aphids. Once a luteovirid is acquired, aphids remain viruliferous for their entire lives (reviewed in

63 (Gray et al., 2014)).

64 The vector manipulation hypothesis has been proposed to explain the evolution
65 of strategies that optimize the plant-to-plant spread of pathogens by vectors through
66 influencing the plant host selection and feeding behavior of the insect vector (Ingwell et
67 al., 2012, Mauck et al., 2012). It is known that both persistent and nonpersistent viruses
68 alter the host plant to enhance transmission by insect vectors, but they use different
69 strategies consistent with their mode of transmission. For instance, aphids are attracted
70 to plants infected with persistent and non-persistent viruses, but upon feeding, they
71 perceive plants infected with a nonpersistent virus as a poor source of food and only
72 transiently probe before finding another host plant (Mauck et al., 2012, Mauck et al.,
73 2010, Alvarez et al., 2007, Castle et al., 1998). However, this brief interaction is
74 sufficient for virions to bind the stylet and be carried to the next host. Other effects of
75 vector manipulation by circulative viruses have been extensively reported, such an
76 increase in longevity and reproduction rates (Castle & Berger, 1993, Pickett et al., 1992,
77 MacKinnon, 1961). It has been suggested that insect vectors and the viruses they
78 transmit collaborate in fighting or avoiding host plant defenses (Hodge & Powell, 2008,
79 Hodge & Powell, 2010, Jiu et al., 2007, Kersch-Becker & Thaler, 2014).

80 In addition to interactions with plant viruses, aphids, like the majority of other
81 hemipteran insect vectors, also harbor close associations with both obligate and
82 commensal microbes (Baumann, 2005, Guyomar et al., 2018) as well as insect
83 pathogens, such as insect viruses (Feng et al., 2017). For aphids and *M. persicae* in
84 particular, these associations include an obligate bacterial endosymbiont, *Buchnera*
85 *aphidicola* (phylum gamma-Proteobacteria) (Baumann et al., 1995). Aphids depend on

86 *Buchnera* to provide the essential amino acids that aphids cannot synthesize or obtain
87 from their diet of phloem sap (Hansen & Moran, 2011). Amino acid transporters are
88 found in high abundance in the bacteriocytes, specialized insect cells harboring the
89 symbiont using proteomics (Poliakov et al., 2011). Different genotypes of *Buchnera*
90 have been found in aphid clones that differ in their ability to transmit poleroviruses in the
91 plant virus family *Luteoviridae* (Cilia et al., 2011). It is unlikely that *Buchnera* plays a
92 direct role in plant virus transmission (Bouvaine et al., 2011), but it is unknown how
93 plant infection with aphid-transmitted viruses influences the aphid-*Buchnera* symbiosis.
94 Aphid-infecting viruses have also been identified and characterized (Gildow & D'arcy,
95 1990, Williamson et al., 1988, Teixeira et al., 2016, van Munster et al., 2003b, Ryabov
96 et al., 2009, Ryabov, 2007, van Munster et al., 2002, van der Wilk et al., 1997),
97 including viruses which have integrated into the aphid genome (Clavijo et al., 2016). In
98 contrast to the luteovirids, which do not replicate in their insect vectors (Day, 1955,
99 Eskandari, 1979, Harrison, 1958, Weidemann, 2009), insect viruses replicate in insect
100 cells and produce effects on aphid physiology that alter phenotypes important to the
101 transmission of plant viruses, such as increasing wing production (Ryabov et al., 2009)
102 or decreasing fecundity (van Munster et al., 2003b, Moon et al., 1998). One aphid-
103 infecting virus is *Myzus persicae densovirus* (MpDNV), a single stranded DNA virus in
104 the family *Parvoviridae* (van Munster et al., 2003b) with a genome of approximately
105 5.7kb (van Munster et al., 2003a). Only minor effects of MpDNV on aphid reproduction
106 and development have been reported (van Munster et al., 2003b). MpDNV is
107 horizontally transmitted via saliva and honeydew, and can also be transmitted
108 transovarially (van Munster et al., 2003b). Interactions with insect-infecting viruses may

109 complicate the interaction of aphids and aphid-borne plant viruses, as both insect and
110 plant viruses require aphids for transmission, but in fundamentally distinct ways. The
111 role insect-infecting viruses play in insect-vectored plant virus transmission remains
112 hitherto unknown, as well as the molecular mechanisms involved in these
113 manipulations.

114 Based on the well-studied manipulation of insect vector feeding behavior by plant
115 viruses, we hypothesized that plant viruses induce changes in biochemical pathways in
116 their insect vectors and sought to compare these effects on *M. persicae* using small
117 RNA sequencing (sRNA-seq) after aphids acquire plant viruses transmitted in two
118 different modes: nonpersistent (PVY) versus persistent (PLRV). sRNA-seq is a powerful
119 tool that can capture the RNAi pathways involved in host post-transcriptional gene
120 regulation as well as antiviral immunity, which is largely mediated by sRNA in plants and
121 invertebrates, such as aphids (Aliyari et al., 2008). The pathways that regulate RNAi are
122 expanded in aphids (Jaubert-Possamai et al., 2010) and also functional (Jaubert-
123 Possamai et al., 2007, Mutti et al., 2006, Pitino et al., 2011). Viruses replicating in host
124 tissues would cause the host to produce virus-derived small interfering RNA (viRNA),
125 which can be detected via sRNA-seq. We anticipated the aphids will launch an sRNA-
126 mediated antiviral response against MpDNV, an animal virus infecting aphids in our
127 colony, but not against PVY or PLRV, two plant viruses which do not replicate in the
128 aphid vector. Our results show that feeding on plants infected with PLRV and PVY
129 cause differing effects on post-transcriptional gene regulation, symbiosis with *Buchnera,*
130 and the antiviral immune response of aphids to MpDNV, an aphid-infecting virus.
131

132 **METHODS**

133 **Aphids and viruses**

134 sRNA-seq was performed on *M. persicae* exposed to plants infected with viruses
135 that varied in their transmission modes (PLRV and PVY). Both plant and aphid samples
136 were collected for sRNA seq. For all experimental conditions, aphids were placed on
137 their source plant tissue or control treatments for three days, transferred to turnip for gut
138 clearing and then collected for sRNA seq (Fig S1). Gut clearing was used for all
139 treatments because a previous experiment performed with no gut clearing prior to
140 sequencing detected abundant plant-derived PLRV reads in aphid samples (Ju and
141 Gray, unpublished data), presumably derived from sRNA ingested from the plant sap
142 during feeding.

143 For these experiments, parthenogenic colonies of the green peach aphid *Myzus*
144 *persicae* Sultz were maintained on caged *Physalis floridana* at 20°C with an 18-hour
145 photoperiod. This *M. persicae* clone was originally collected from New York and
146 maintained in the lab clonally for over 15 years. Aphids were allowed a three-day virus
147 acquisition access period (AAP) on the following treatments prior to collecting aphids for
148 sRNA-seq (Fig. S1): 1) PLRV-infected potato plants, cv. Red Maria; 2) purified, 50 µg/µl
149 infectious purified PLRV in 30% sucrose; 3) PVY-infected potato plants, cv. Goldrush; 4)
150 mock inoculated potato plants, cv. Red Maria and 5) 30% sucrose solution. After the
151 AAP, aphids were transferred to turnip plants, cv. Purple Top White Globe, (a nonhost
152 for PLRV and PVY) for three days to clear all insect tissues of plant viRNAs mapping to
153 PLRV and PVY produced *in planta*. Aphids were harvested from turnip plants and flash-
154 frozen for sRNA isolation. For each treatment, three to four biological replicates were

155 harvested, each containing a pool of approximately 700 aphids (50-80mg). To ensure
156 that aphids acquired PLRV from the infected plants and the virus-laden diets, a subset
157 of aphids were tested by RT-PCR, using primers that amplify a 660bp fragment of
158 PLRV, which included the coat protein: (5'-CTAAAGATTTCCTCCCACGTGCG-3') and
159 (5'-GGAGTGGGTGTTGGTTGTGGGC-3').

160 Tissue was also collected from turnip plants used to gut clear aphids exposed to
161 PLRV (PLRV-infected potato and purified PLRV treatments). Potato and turnip plant
162 samples were collected from aphid-inoculated leaves three days post inoculation (DPI)
163 and from systemically PLRV-infected potato leaves three weeks post inoculation (WPI).
164 Turnip samples were only collected three days after PLRV inoculation by aphids
165 because turnip does not become locally or systemically infected with PLRV, so
166 sampling at later time points for systemic infection was not necessary.

167 Three-week-old hairy night shade (*Solanum sarrachoides,* HNS) plants were
168 inoculated with a cDNA clone of PLRV wild type (Franco-Lara et al., 1999) to serve as
169 source of virus for inoculation of potato plants by aphid feeding. Tobacco (*Nicotiana*
170 *tabacum*) plants infected with PVY strain O (Karasev et al., 2011) were used as
171 inoculum for aphid transmission of PVY to the potato plants used in the experiments.
172 HNS plants were used as a source of virus because they are more easily inoculated
173 with the cDNA clone in *Agrobacterium tumefaciens* (DeBlasio et al., 2015).
174

175 **sRNA isolation, library construction and sRNA sequencing**

176 Small RNAs were isolated from whole aphids and plant leaves using the
177 mirPremier microRNA isolation kit (Sigma-Aldrich). RNA integrity was confirmed using

178 gel electrophoresis. Small RNA libraries were constructed from 50-100 ng of sRNA, as
179 described (Chen et al., 2012), with some modifications. A commercial small RNA 3'
180 linker was used for adapter ligation (5'rApp-CTGTAGGCACCATCAAT-Amine 3') (New
181 England BioLabs). The reverse transcription primer 5'Amine-
182 GACGTGTGCTCTTCCGATCT ATTGATGGTGCCTACA*G 3' was used to hybridize to
183 the excess 3' adapter and convert the single stranded DNA adapter into a double-
184 stranded DNA molecule. Three to four individual sRNA libraries were prepared for each
185 aphid and plant treatment from purified sRNA using unique barcoded-adapters.
186 Individual libraries were separated by gel electrophoresis and 160-180bp sized libraries
187 were selected, as the adapter is 141bp. Libraries were pooled and quality checked with
188 a bioanalyzer. Libraries were then pooled in four lanes and sequenced on an Illumina
189 HiSeq2500 instrument at the Cornell Biotechnology Resource Center, operating in "High
190 Output Mode" with single-end 50bp read length.
191

192 **sRNA Data Analysis**

193 sRNA deep sequencing data were processed to remove sequencing adapters,
194 low quality reads, and short reads (<15 nt) using the sRNA clean script provided by
195 VirusDetect (Zheng et al., 2017). The remaining reads were aligned to a ribosomal RNA
196 database (Quast et al., 2013) using Bowtie (Langmead et al., 2009) and the mapped
197 rRNA reads were removed. The cleaned sRNAs were mapped to the reference
198 genomes using Bowtie (Langmead et al., 2009) allowing up to 1 mismatch to account
199 for differences between the reference sequences and our aphid clone and virus strains.
200 Reference genomes included: *Potato leafroll virus* (NC_001747 and KC456053),

201 *Buchnera aphidicola* F009 strain from *Myzus persicae* (CP002703), *Myzus persicae*
202 *densovirus* (AY148187), *Potato Virus Y* (EF026074), and *Myzus persicae* G006 (draft
203 genome available at aphidbase.org). The mapping depth at each position of the *Myzus*
204 *persicae densovirus* (MpDNV) genome was generated using SAMtools (Li et al., 2009).
205 The cleaned reads were also aligned to the mature tRNAs of *B. aphidicola* using Bowtie
206 with 0 mismatches, and the resulting alignments were visualized using Tablet (Milne et
207 al., 2013).

208 To look for piRNA, sRNA reads of 26-27nt from aphids exposed to PLRV were
209 aligned to the *M. persicae* G006 draft genome using Bowtie allowing no mismatch.
210 Mapped reads of 26 and 27 nt were analyzed using the piRNN deep learning algorithm
211 (Wang et al., 2018) using the *Drosophila melanogaster* model, since this is the best
212 available model for insects. Sites of integrated MpDNV was obtained by aligning the *M.*
213 *persicae* draft genome G006 to the genome of MpDNV (AY148187) using BLAST
214 (Altschul et al., 1990), with an e-value cut-off of 10^{-5}.

215 To observe differences in the size distribution of reads mapping to the *M.*
216 *persicae* (Fig. 2) or MpDNV (Fig. 4) genome, the percentage of reads of each size
217 aligning to the reference genome was averaged across biological replicates. Error bars
218 represent one standard error. We compared the distributions of sRNA sizes from the
219 different treatments using methodology based on Kramer (Kramer, 2014), modified for
220 multinomial distributions, which allowed us to include multinomial sampling error
221 variance, replicate-to-replicate variance, and treatment-to-treatment variance. The
222 within-treatment variance was created by simulating each replicate within a treatment
223 (e.g. treatment A) from a multinomial distribution using the proportion of sRNA sizes and

224 counts from that replicate and building the null distribution from means (based on four
225 replicates) of the log of sum-of-square differences, with each difference based on two
226 simulated reps. This was done 1000 times using all replicates of treatment A, providing
227 the null distribution of within-treatment mean differences. The mean of the log of sum-
228 of-square differences between simulated data from all replicates of two different
229 treatments (e.g. treatment B versus treatment A) was then compared to the null
230 distribution of means built from only treatment A simulated data. If this mean lay outside
231 the upper 95th percentile of the within treatment A distribution, the distributions of sRNA
232 sizes from treatment B was declared to differ significantly from that of treatment A. The
233 p-values were also calculated using treatment B to generate the null distribution and in
234 all cases gave similar p-values to those from a treatment A null distribution.
235 To compare the abundance of reads across treatments, a one-way fixed effects
236 ANOVA was performed. Tukey's Honest Significant Difference (HSD) test was used to
237 perform pairwise comparisons if the ANOVA test was significant. The assumption of
238 normality was checked using the Shapiro-Wilk test and a normal probability plot. The
239 assumption of homoscedasticity was checked using the Bartlett test. All statistical tests
240 were performed in R (R Core Team, 2017).
241

242 **Quantifying MpDNV titer in aphids allowed an AAP on PLRV-infected or**
243 **uninfected plants**

244 To test whether PLRV infection in plants impacted MpDNV titer in aphids, we
245 used droplet digital PCR (ddPCR) to measure MpDNV titer in aphids. Aphids were given
246 a three day AAP on PLRV-infected or uninfected hairy nightshade (*Solanum*

247 *sarrachoides,* HNS) plants. DNA was extracted from single aphids (20
248 replicates/treatment), by homogenizing the whole aphid using a micro pestle in 30 µL of
249 extraction buffer (0.01M Tris pH 8.0, 0.001M EDTA and 0.025M NaCl) containing
250 0.006% Proteinase K. The insect homogenate was then incubated at 37°C for 30
251 minutes (Proteinase K digestion) followed by 95°C for 2 min (Proteinase K heat
252 inactivation). After Proteinase K treatment, the samples were centrifuged for 7 min at
253 16,100 x g. The supernatant was then transferred into a new tube and stored at -20°C
254 until further use. A droplet digital PCR (ddPCR) assay was developed for MpDNV using
255 the QX100 droplet digital PCR system (Bio-Rad). The ddPCR reaction for MpDNV
256 consisted of 10 µL of 2X ddPCR Evagreen SuperMix (Bio-Rad), 1 µL of each 10 µM
257 MpDNV primers (5'-TGACAATGGGTATATTCATTGACCT-3' and 5'-
258 ATCGTGCGTCAAAAGAAACCCT-3'), 7 µL of dH2O and 2 µL of DNA diluted at 1:800
259 in a final volume of a 20 µL reaction. A cartridge holder containing 20 µL of the ddPCR
260 reaction and 70 µL of droplet generator oil for Evagreen (Bio-Rad) was placed into the
261 QX100 droplet generator (Bio-Rad) where 40 µL droplets were generated. Droplets
262 were then transferred to a 96-well plate (Eppendorf) and the plate was sealed with an
263 easy pierce foil seal (Bio-Rad). PCR amplification was carried out on the Applied
264 Biosystems 2720 Thermocycler. The thermocycling conditions started at 95°C for 5 min,
265 followed by 40 cycles of 95°C for 30 sec and 60C for 1 min, 1 cycle at 4°C for 5 min, 1
266 cycle at 90°C for 5 min and ending at 12°C. Following amplification, the plate was
267 inserted into the droplet reader cassette and loaded into the droplet reader (Bio-Rad).
268 The droplets were automatically read at a rate of 8 wells per 15 min. The ddPCR droplet
269 data was analyzed using the QuantaSoft analysis software (Bio-Rad), which presents

the target results as copies per µL of PCR mixture. The number of copies of MpDNV per µL was compared between treatments using the Kruskal-Wallis nonparametric test, since the Shapiro-Wilk test for normality was significant ($p < 0.0001$).

MpDNV titer in aphids allowed an AAP on the PLRV silencing suppressor protein, P0

We investigated if the PLRV silencing suppressor P0 was responsible for the increase in MpDNV titer in PLRV-viruliferous aphids using *Nicotiana benthamiana*, which is a host of both PLRV and *M. persicae* and commonly used for transient protein expression in the leaves. To test this hypothesis, aphids were fed upon *N. benthamiana* tissue transiently expressing PLRV, P0, or GFP driven by a 35S promoter or non-infiltrated (healthy) plants. Transient expression was achieved using plant inoculation by *Agrobacterium tumefasciens* as described . Synchronized fourth instar aphids were placed upon infiltrated leaves one DPI, caged on 3 leaves/plant, 5-6 plants/treatment. One cage of aphids per plant was collected in pools of 4-8 aphids, resulting in 10-12 biological replicates per treatment per time point. Insects were homogenized by cryogenic grinding in liquid nitrogen for 6 minutes at 25 Hz with a Mixer Mill MM 400 (Retsch). DNA was extracted using 150 µL extraction buffer with Proteinase K treatment, as described above. DNA samples were normalized to 5 ng/µL and then diluted 1:8. MpDNV titer was quantified using the ddPCR assay described above. The number of copies of MpDNV per µL was compared among treatments using a one-way fixed effects ANOVA for the first time point (1 day, 2 DPI), and via the Kruskal-Wallis nonparametric test for the second time point (3 days, 4 DPI), since the Shapiro-Wilk test

293 for normal distribution was significant ($p < 0.05$). Titers are presented as copies of
294 MpDNV found in 1ng/µL of total aphid DNA (Fig. 6).
295 To assess silencing suppressor activity in the plant, as previously described
296 (Shen et al., 2010), *N. benthamiana* plants were co-infiltrated with *A. tumefaciens*
297 cultures expressing GFP, double-stranded GFP, and P0 or WT PLRV. Double-stranded
298 GFP will silence GFP expression and result in no GPF fluorescence, unless silencing
299 suppression occurs. GFP expression and therefore silencing suppressor activity was
300 accessed using a UV lamp 4 DPI. The P19 silencing suppressor protein from *Tomato*
301 *bushy stunt virus* was included as a positive control, and no silencing suppressor for a
302 negative control. Transient expression of all proteins was driven by the 35S promoter.
303

304 **MpDNV titer in winged and non-winged aphids**

305 To see if there was a correlation between densovirus and winged morphs, as has
306 been observed in other aphid species (Ryabov et al., 2009), we quantified MpDNV in
307 winged and non-winged aphids. Alates and apterous aphids were collected at the same
308 time from the same colony on uninfected *Physalis floridiana* (pools of 5 aphids, 16
309 replicates per treatment). DNA was extracted using cryogenic lysis of aphid tissue and
310 extraction buffer as described for aphid feeding upon P0. DNA samples were
311 normalized to 5 ng/µL and then diluted anywhere from 1:8 to 1:200, depending on
312 MpDNV titer in the sample as a result of the incredible range of MpDNV titer found in
313 winged aphid samples. Therefore, data are presented as copies of MpDNV found in
314 1ng/µL of total aphid DNA. Average MpDNV titer was compared using the Mann-
315 Whitney nonparametric test ($p = 9.57 \times 10^{-5}$) as data were found to be not normally

316 distributed via the Shapiro-Wilk test ($p = 1.70 \times 10^{-6}$) and heteroscedastic via the
317 Levene test ($p = 0.014$).
318
319 **Localization of MpDNV in PLRV-viruliferous aphids by Fluorescence *In Situ***
320 **Hybridization**
321 Fluorescence *In Situ* Hybridization (FISH) was performed as previously
322 described (Kliot et al., 2014). Briefly, specimens were fixed in Carnoy's fixative
323 (chloroform-ethanol-glacial acetic acid, 6:3:1, vol/vol) for 5 min following gut dissection
324 in 1x PBS and hybridized overnight in hybridization buffer (20 mM Tris-HCl, pH 8.0, 0.9
325 M NaCl, 0.01% [wt/vol] sodium dodecyl sulfate, 30% [vol/vol] formamide) containing 10
326 pmol fluorescent probe per uL. For specific targeting of PLRV and MpDNV, PLRV (5′-
327 TTTCCATTTCCCTTCCACAG-3′) (Ghanim et al., 2009) and DenR2 (5′-
328 ATCGTGCGTCAAAAGAAACCCT-3′) DNA probes were used respectively. Nuclei were
329 stained with 4′,6′-diamidino-2-phenylindole (DAPI; 0.1 mg ml^{-1}). The stained guts were
330 mounted in hybridization buffer and viewed under a Leica TCS-SP5 (Leica
331 Microsystems Exton) confocal microscope. At least 10 guts were viewed for each
332 treatment under the microscope to confirm reproducibility. Specificity of detection was
333 confirmed using no-probe and PLRV-free controls.
334
335 **RESULTS & DISCUSSION**
336 **Small RNA sequencing detected an sRNA-mediated antiviral immune response to**
337 **PLRV in potato, a host of PLRV, but not in turnip, a non-host, or *M. persicae,* the**
338 **aphid vector.** Aphids were allowed an AAP on PVY-infected potato plants, PLRV-

339 infected potato plants, purified PLRV virions delivered via a sucrose diet, and a purely
340 sucrose diet (Fig. S1). After a three-day AAP, aphids were transferred to turnip plants
341 for three days for gut clearing. Potato plant and turnip plant samples were collected
342 from aphid-inoculated leaves three DPI and from systemically infected potato leaves
343 three WPI (Fig. S1). Three to four individual sRNA libraries were prepared for each
344 aphid and plant treatment from purified sRNAs using unique barcoded-adapters. Each
345 aphid library generated between 3 and 7 million reads, while the plant libraries
346 generated between 1 and 2 million reads (Table 1). Aphid and plant libraries generated
347 reads varying from 15 to 40 nt in length, which we refer to in this manuscript as small
348 RNA (sRNA) reads.

349 viRNA reads that aligned to the PLRV genome were present in PLRV-infected
350 potato at both sampling times (Table 1). The number of viRNA reads that aligned to
351 PLRV in potato at three DPI was lower than at three WPI, but still readily detectable,
352 which indicates that three days is sufficient time to detect PLRV viRNA in plant tissue.
353 The majority of those reads were 21-22 nt (Fig. S2), which is in the range of the viRNA
354 size reported for plants, including potato (Kutnjak et al., 2015, Hwang et al., 2013, Li et
355 al., 2012). In contrast, the turnip plants used for gut clearing of aphids did not produce a
356 significant number of PLRV-derived sRNA (Table 1), which is consistent with the fact
357 that turnip is a non-host of PLRV. Therefore virus replication does not occur in turnip.

358 No sRNA reads that aligned to the PLRV genome were detected in aphids
359 allowed an AAP on PVY-infected plants and all control treatments (sucrose diet and
360 mock-inoculated potato). Minimal sRNA reads mapping to PLRV were generated in
361 aphids which acquired PLRV from PLRV-infected plants or purified PLRV diet

362 treatments (Table 1). These reads were manually inspected and are considered false
363 positives, as they could also be aligned to other, non-PLRV sequences ranging from
364 aphids, humans, and plants. Similarly, the minimal sRNA reads mapping to the PVY
365 genome in aphids represented false positive as well (Table 1). These results are
366 consistent with the fact that PLRV is transmitted by *M. persicae* in a non-propagative
367 manner (Day, 1955, Eskandari, 1979, Harrison, 1958, Weidemann, 2009). Furthermore,
368 this result shows that gut clearing was effective at removing the majority of plant-derived
369 sRNA from the aphid samples. The validity of our approach is confirmed by these
370 controls, and enables us to observe novel sRNA interplay between the plant viruses and
371 the aphid, as well as the relationship with the aphid obligate endosymbiont and an
372 insect-infecting virus, as further described below.
373
374 **PLRV, but not PVY, altered the size distribution of sRNA mapping to the aphid**
375 **genome, including an increase in piwi-interacting RNA (piRNA).** To test whether
376 PVY and PLRV had an impact on the size distribution of *M. persicae*-derived small
377 RNAs, we aligned the sRNA reads to the *M. persicae* genome. We found the
378 distribution of *M. persicae*-derived sRNA to be distinct from all other treatments when
379 aphids acquired PLRV, regardless of source (from infected plants or purified PLRV in
380 sucrose diet, $p < 0.001$, Fig. 1). In aphids from the mock-inoculated potato treatment, a
381 sucrose diet without PLRV, or PVY-infected plants, the most abundant size of siRNA
382 was 22 nt. The 22 nt size may be the more abundant size for siRNAs produced in
383 aphids, as this is also the dominant size produced by the cotton melon aphid, *Aphis*
384 *gossypii* (Sattar et al., 2012). Fewer 22 nt siRNA matching the *M. persicae* genome

385 were generated in aphids allowed an AAP on PLRV-infected plant tissue compared to
386 those with an AAP on PVY-infected potato plants (Tukey's HSD test, $p = 0.0141$), mock-
387 inoculated potato ($p = 0.0029$), and pure sucrose diet ($p = 0.0067$). Interestingly, this
388 decreased number of 22-mers was also observed for aphids feeding on purified PLRV
389 (Tukey's HSD test, $p = 0.0147$, $p = 0.0030$, $p = 0.0070$, Fig 1). In a total of 20 pairwise
390 comparisons for all treatments, aphids which had acquired PLRV from PLRV-infected
391 plants or purified PLRV showed a significant increase in 26 and 27 nt sRNA (Tukey's
392 HSD test, $p < 0.05$, Fig. 1), which is in the range of piRNAs (Luteijn & Ketting, 2013).
393 Over 90% of these 26 and 27-mer reads in our study were predicted to be piRNA (Tabl
394 S1) by analyzing them with the piRNN deep learning algorithm (Wang et al., 2018).
395 piRNA are often produced in the germ line (Luteijn & Ketting, 2013). It is well known that
396 feeding on PLRV-infected plants increases the fecundity of *Myzus persicae* (Castle &
397 Berger, 1993), a form of vector manipulation. Therefore, this observed increase in 26-27
398 mers may be the result of an increase in germ tissue, and as such, may serve as a
399 molecular indicator of that vector manipulation by the virus. A nearly identical plasticity
400 in the sRNA response of aphids has previously been observed in the aforementioned
401 study on *A. gossypii* (Sattar et al., 2012). In that study, *A. gossypii* were exposed to
402 melon lines expressing the virus aphid transmission (VAT) gene, which is an CS-NBS-
403 LRR R gene and imparts resistance to melon against aphid feeding and several aphid-
404 transmitted plant viruses. Aphids feeding on the VAT+ melon lines also produced an
405 increase in 26- and 27-mers in the aphid (Sattar et al., 2012). Sattar and colleagues
406 also provided evidence that this longer class of sRNA was enriched for piRNAs in *A.*
407 *gossypii.* In their study, over 46% of the reads in this size class were enriched for

408 transposable elements, a common feature of piRNA sequences in *Drosophila* and other
409 animals (Brennecke et al., 2007). It is intriguing that the purified PLRV treatment in our
410 study elicited a similar response in the aphid as feeding on plants expressing an anti-
411 viral, anti-aphid immunity R-gene. Collectively, these results suggest that plant viruses
412 can prime the aphid's piRNA pathways through germ-line reprogramming in the
413 absence of the plant in a manner similar to the expression of plant R-genes.
414
415 **Exposure to the plant virus PLRV also altered the aphid's relationship with its**
416 **obligate endosymbiont, *Buchnera aphidicola.*** *B. aphidicola* contributes to the
417 aphid's nutritional needs, providing the essential amino acids that the aphid is unable to
418 synthesize or obtain from its diet in sufficient amounts (Hansen & Moran, 2011).
419 Differential expression of genes in amino acid biosynthesis pathways between
420 bacteriocytes and other aphid tissues indicate complementarity between amino acid
421 pathways encoded by the host and symbiont genomes (Hansen & Moran, 2011).
422 However, it is not known how *Buchnera* regulates gene expression, as *Buchnera* has
423 lost most of the genes for transcriptional regulation that are present in free-living
424 relatives, a feature common of endosymbiont genomes (Shigenobu et al., 2000). We
425 found that about nine percent of the sRNAs from aphid samples aligned to genes from
426 *B. aphidicola* (Table 1), which was slightly more than what was reported in the Sattar et
427 al. study (Sattar et al., 2012). Among these *Buchnera* reads in our study, approximately
428 12% were derived from aminoacyl-tRNAs (Table 1), with asparagine being the most
429 abundant aminoacyl-tRNA represented (Asn-tRNA). These reads are consistent with a
430 novel class of sRNA, called tRNA fragments (tRFs), which have been found to be not

431 only present, but abundant in both prokaryotes and eukaryotes (Sobala & Hutvagner,
432 2011). The tRFs are products of precise tRNA processing rather than random
433 degradation (Lee et al., 2009). They are often produced by non-dicer nucleases and can
434 be classified as 5', 3', and central fragments with respect to the mature or precursor
435 tRNAs from which they are derived. In our data, the alignments of the small RNA
436 sequences to the tRNAs were not random, but rather showed distinct distributions for
437 each tRNA. For example, reads for Asn-tRNA aligned to the 5'end of the RNA and
438 some to the 3' end, Arg-tRNA had reads mapping to the middle of the RNA, and Leu-
439 tRNA had reads mapping to the 3' end of the gene (Fig. S3). The distribution of these
440 reads along the mature tRNA did not change with treatment; only their relative
441 abundance changed. The observation that these reads map to precise regions of the
442 tRNA rather than being randomly dispersed leads us to believe that we are capturing
443 actual tRNA-derived sRNA rather than degradation products of tRNAs. It is unknown,
444 but possible, that the tRFs and sRNAs mapping to other *B. aphidicola* genes we
445 detected represent a means of tRNA gene regulation in this endosymbiotic bacterium.
446 In other systems, tRFs were previously shown to perform regulatory roles and
447 cleavage of tRNA is often induced by stressors, such as amino acid starvation
448 (Thompson & Parker, 2009). tRFs have even been found to associate with Argonaute
449 proteins and may perform a silencing role similar to siRNAs or miRNAs (Sobala &
450 Hutvagner, 2011). In *Acyrthosiphon pisum* (the pea aphid), a significant correlation was
451 reported between tRNA relative abundances and codon composition of *Buchnera* genes
452 and tRNA abundances also changed during nutritional stress (Charles et al., 2006). In
453 our data, the proportion of sRNA aligned to each *Buchnera* aminoacyl-tRNAs varied

454 across treatments (Table S2). Aphids on the sucrose diet treatment lacking PLRV and
455 on PVY-infected potato produced significantly more sRNAs mapping to Asn-tRNA than
456 aphids given an AAP on PLRV-infected potato plants (Fig. 2A). These data suggest that
457 the amino acid requirements of aphids feeding on an unbalanced sucrose diet are
458 similar to that of aphids given an AAP on PVY-infected potato and are in agreement
459 with previous studies showed that aphids perceive a plant infected with a non-persistent
460 virus as a low quality diet (Mauck et al., 2012, Mauck et al., 2010). In contrast, for most
461 of the other aminoacyl-tRNAs with an abundant number of reads, such as Ser, Leu, and
462 Gln, the proportion of sRNAs found in aphids given an AAP on a PLRV source (either
463 diet or infected tissue) was higher, compared to aphids given an AAP on a sucrose diet
464 lacking PLRV, mock-inoculated potato or on PVY-infected potato (Fig. 2). These data
465 indicate that PLRV causes much greater effects on the relative abundance of tRFs than
466 PVY does, and may therefore have a greater effect on the relationship between the
467 aphid vector and *B. aphidicola.*
468
469 **PLRV altered the relationship of *M. persicae* with the insect-infecting virus**
470 **MpDNV.** In our aphid colony, MpDNV was visualized using fluorescent *in situ*
471 hybridization (FISH) and detected along the entire alimentary canal including the
472 posterior midgut, which is the site of PLRV acquisition (Fig. S4). Qualitatively, no
473 obvious change in virus distribution or abundance was observed between aphids given
474 an AAP on uninfected or PLRV-infected plants. In other studies icosahedral particles of
475 MpDNV were reported to localize in the cytoplasm of the aphid stomach cells but not
476 the posterior midgut or hindgut cells (van Munster et al., 2003b). It is possible that

477 different strains of MpDNV have different tropisms to regions of the gut in *M. persicae.*

478 Aphids, including *M. persicae*, encode homologs for all core genes of antiviral
479 defense pathways, such as the Toll signaling, JAK-STAT, and viRNA pathways
480 (Gerardo et al., 2010). The genes involved in the sRNA pathway, *dcr-2*, *ago-2,* and
481 *r2d2*, are present in single copies in the pea aphid genome (Jaubert-Possamai et al.,
482 2010). The machinery involved in the viRNA pathway has been shown to be functional
483 via RNA interference in aphids and other insects (Jaubert-Possamai et al., 2007,
484 Jaubert-Possamai et al., 2010, Pitino et al., 2011, Sapountzis et al., 2014, Whyard et
485 al., 2009). Thus, it was not surprising that several thousand sRNA reads from all aphid
486 samples aligned to the genome of the insect-infecting MpDNV (GenBank Acc. No
487 AY148187, Table 1), with these viRNA ranging from 15 to 40 nt in length. The size
488 distribution of viRNAs in aphids allowed an AAP on PLRV-infected potato plants was
489 unique compared to other treatments ($p < 0.001$, Fig. 3), with an abundance of
490 unusually long sRNAs of 35 to 40 nt. To test whether the variance in the distribution
491 could be derived from sRNAs within this unusual size range, a total of 36 pair-wise
492 comparisons were performed for sRNAs in this size range for all treatments. All sRNAs
493 in the 35-40 nt size range in aphids which had acquired PLRV from infected plants had
494 a significantly higher relative abundance compared to all other treatments (Tukey's
495 Honest Significant Difference (HSD) test, $p < 0.05$). These unusually long reads may be
496 due to incomplete cleavage of viRNA precursors or may be other degradation products
497 of viral transcripts. For most of the other treatments, the most abundant size of MpDNV
498 viRNA reads was 22 nt, which is in the range of the most common size of sRNA
499 generated by Dcr-2 in insects (Sabin et al., 2013, Xu et al., 2012, Aliyari et al., 2008).

500 The number of 22 nt viRNAs was significantly lower in aphids given an AAP on PLRV-
501 infected plants compared to mock-inoculated potato (Tukey's HSD test, $p = 0.0379$),
502 similar to the reduction of 22-mer *M.* persicae-derived sRNA reported above for this
503 same treatment. The distribution of viRNA was also distinct for aphids given an AAP on
504 purified PLRV ($p < 0.001$, Fig. 3) compared to all other treatments, for which the most
505 abundant sizes were 17 and 22 nt, though this treatment did not exhibit the same
506 unusually long sRNA as the aphids given an AAP on PLRV-infected plants, or less 22-
507 mers compared to aphids given an AAP on mock-inoculated potato (Tukey's HSD, $p =$
508 0.1977).

509 Sequencing of *M. persicae* reveals integrations of densovirus-like sequences
510 (DLSs) into the aphid genome (Clavijo et al., 2016). The integrated viral sequences
511 have been shown to be transcribed in *M. persicae,* generating amino acid sequences
512 that share 33 to 51% identity with MpDNV proteins (Clavijo et al., 2016). To check
513 whether the sRNAs obtained in our experiments were in the sites of integration of
514 MpDNV sequences into the *M. persicae* genome, we generated a consensus sequence
515 for the MpDNV genome and aligned it to the *M. persicae* genome and found seven
516 regions with high similarity, based on a e-value cut-off of $< 10^{-5}$. Four of these regions
517 matched to the *M. persicae* genome with 100% similarity (Table S3). We mapped the
518 distribution of sRNA reads along the MpDNV genome and found no preference for
519 these regions of integration (Fig. S5). Since these regions with high similarity
520 sequences to the aphid genome were not overrepresented in our sRNA dataset, it is
521 likely that the sRNA reads mapping to MpDNV represent an actual antiviral response of
522 aphids to MpDNV infection.

523 Considering that exposure to a PLRV-infected plant altered the aphid sRNA-
524 mediated antiviral immune response, we wanted to test if PLRV infection in plants also
525 altered MpDNV titer. MpDNV was quantified in single aphids allowed an AAP for three
526 days on PLRV-infected and uninfected HNS plants (20 replicates/treatment). Aphids
527 allowed an AAP on PLRV-infected HNS plants had significantly more copies of MpDNV
528 than aphids placed on the uninfected HNS plants (Kruskal-Wallis test, $p = 0.02$, Fig 4A).
529 While we do not know if this increase in MpDNV titer in the aphid is a direct result of the
530 aforementioned changes in the viRNA profile caused by exposure to PLRV-infected
531 plants, these data suggest that PLRV causes two important changes to the aphid
532 antiviral immune response against MpDNV.

533 In an attempt to identify which PLRV proteins were causing this effect on *M.*
534 *persicae,* we tested the effect of P0 on MpDNV titer. P0 is the silencing suppressor
535 protein encoded by PLRV and other virus in the genus *Polerovirus,* that marks AGO1
536 for degradation in the plant host (Baumberger et al., 2007, Bortolamiol et al., 2007).
537 Non-viruliferous (with no PLRV) aphids were placed on four different plant treatments
538 for one day and three days: 1) *N. benthamiana* leaves transiently expressing the WT
539 infectious clone of PLRV, 2) leaves expressing only the PLRV P0 protein, 3) leaves
540 expressing a green fluorescent protein (GFP) control and 4) uninfected leaves (healthy
541 control). No significant differences in MpDNV titer were found among the four
542 treatments after 1 day (Fig. 4B, top). After three days (corresponding to 4 DPI), MpDNV
543 titer was highest in aphids on the P0 treatment compared to all other treatments,
544 including aphids fed on the PLRV-infected leaves, which would presumably also contain
545 P0 expressed in the context of viral infection (Fig. 4B, bottom). There could be many

546 reasons why expressing P0 alone in this experiment leads to an even greater increase
547 in MpDNV than expressing the entire virus. It may be linked to the silencing suppressor
548 activity of these particular constructs. Using a silencing suppressor activity assay (Shen
549 et al., 2010) in *N. benthamiana* we showed that, after three days, the same timepoint
550 used in the aphid experiment, the silencing suppressor activity of P0 expressed alone
551 was higher than P0 expressed in the context of WT PLRV (Fig. S6). Regardless, these
552 data show that expression of the PLRV silencing suppressor P0 in plants, even in the
553 absence of a PLRV infection, induced higher MpDNV titers in the aphid. Thus, the P0
554 protein may be somehow altering the aphid antiviral immune system either directly in
555 aphid cells or indirectly through the plant. Nothing is known as to whether P0 has a
556 function in the aphid. These results raise additional questions about P0 activity in the
557 plant and aphid during viral infection that are beyond the scope of the current study.
558 Aphids are polyphenic. In asexual aphid lineages, both winged and non-winged
559 individuals are produced. In the rosy apple aphid, *Dysaphis plantaginea,* densovirus
560 (DplDNV) infection induces the production of winged morphs (Ryabov et al., 2009).
561 Densovirus-like sequences analogous to DplDNV have been found to be integrated into
562 the *M. persicae* genome, along with sequences from MpDNV (Clavijo et al., 2016).
563 Considering the connection between DplDNV and wing production in *D. plantaginea*, we
564 quantified MpDNV titer in pools of winged and non-winged *M. persicae* individuals. We
565 found the difference in MpDNV titer in winged morphs and non-winged morphs is highly
566 significant, with winged morphs having a significantly higher MpDNV titer (Mann-
567 Whitney test, $p < 0.001$, Fig. 4C) and greater variance in titer (Levene's test, $p = 0.014$).
568 These data establish a correlation between MpDNV infection levels and wing production

569 in this aphid species. Therefore, it is possible that MpDNV promotes wing production in
570 *M. persicae* and this effect is mediated by PLRV to promote plant-to-plant virus
571 dispersal. Gildow (1980) published a seminal paper showing that two aphid species,
572 *Sitobion avenae* and *Rhopalosiphum padi,* reared on plants singly infected with three
573 different species of yellow dwarf viruses showed an increase in the production of
574 winged morphs compared to aphids reared on uninfected plants. Furthermore, he
575 showed that this increase was not related to the acquisition of the virus, but rather due
576 to an unidentified component of the infected plant (Gildow, 1980). Future work is
577 needed to investigate the connection between MpDNV, wing production, and PLRV
578 transmission.
579

580 **Conclusion**

581 These results showed intriguing ways in which the persistent plant virus PLRV
582 alters sRNA-mediated processes in its vector, such as posttranscriptional gene
583 regulation, the relationship with the obligate endosymbiont, and the relationship with a
584 insect-infecting virus, whereas the nonpersistent PVY produced little or no effects on
585 these same processes. However, one important limitation of this study is that the host
586 switch of aphids from potato plants to turnip for gut-clearing during the sRNA-seq
587 experiment may have had an effect on aphid sRNA production and metabolism, as
588 switches between solanaceous and brassicaeous hosts for *M. persicae* have previously
589 been found to alter protein expression (Francis et al., 2006) and PLRV transmission
590 (Pinheiro et al., 2017). However, the host switch to turnip was controlled for in all
591 treatments so that conclusions can be drawn between the effect of the different virus

592 treatments independent of any potential host switch effects on the sRNAs. Different
593 potato cultivars were also used for aphid acquisition of PLRV vs. PVY and may have
594 induced some cultivar-specific changes in the aphids in these two treatments.
595 Understanding the extent to which host switch plays a role in these interactions is an
596 important area of investigation, especially considering how often host switch may occur
597 in the field for a polyphagous vector such as *M. persicae.* Future experiments should
598 also determine to what extent PLRV effects on the aphid antiviral immune system in
599 natural aphid populations, to control for any effects of the *M. persicae* genotype used in
600 our study and to better understand how aphid-infecting viruses may be used as aphid
601 biocontrol agents.
602

603 **ACKNOWLEDGEMENTS**

604 Funding for the present research was provided by NSF grant 1354309 (to MH), an
605 Embrapa Graduate Student Fellowship (to PVP), and an NSF Graduate Research
606 Fellowship DGE-1650441 (to JRW). DNA sequence data for *Myzus persicae* were
607 downloaded from AphidBase, http://www.aphidbase.com/aphidbase/. Funding for
608 *Myzus persicae* clone G006 genomic sequencing was provided by USDA-NIFA award
609 2010-65105-20558.
610 The funders had no role in study design, data collection and interpretation, or the
611 decision to submit the work for publication. The authors gratefully acknowledge Jason
612 Ingram (USDA ARS, Ithaca, NY) for support with pesticide applications, Niaome
613 Hickman (Boyce Thompson Institute, Ithaca, NY) for her assistance with planting and
614 aphid handling and Angela Douglas and Heck lab members for productive discussion

about these results.

DATA AVAILABILITY

The datasets supporting the conclusions of this article have been made available to the research community in the NCBI Short Read Archive (SRA) and can be found under BioProject PRJN514359.

REFERENCES

Aliyari R, Wu Q, Li HW*, et al.*, 2008. Mechanism of induction and suppression of antiviral immunity directed by virus-derived small RNAs in *Drosophila*. *Cell Host Microbe* **4**, 387-97.

Altschul SF, Gish W, Miller W, Myers EW, Lipman DJ, 1990. Basic local alignment search tool. *J Mol Biol* **215**, 403-10.

Alvarez AE, Garzo E, Verbeek M, Vosman B, Dicke M, Tjallingii WF, 2007. Infection of potato plants with *Potato leafroll virus* changes attraction and feeding behaviour of *Myzus persicae*. *Entomol Exp Appl* **125**, 135-44.

Baumann P, 2005. Biology bacteriocyte-associated endosymbionts of plant sap-sucking insects. *Annu Rev Microbiol* **59**, 155-89.

Baumann P, Baumann L, Lai CY, Rouhbakhsh D, Moran NA, Clark MA, 1995. Genetics, physiology, and evolutionary relationships of the genus *Buchnera*: intracellular symbionts of aphids. *Annu Rev Microbiol* **49**, 55-94.

636 Baumberger N, Tsai CH, Lie M, Havecker E, Baulcombe DC, 2007. The Polerovirus
637 silencing suppressor P0 targets ARGONAUTE proteins for degradation. *Curr Biol* **17**,
638 1609-14.

639 Bortolamiol D, Pazhouhandeh M, Marrocco K, Genschik P, Ziegler-Graff V, 2007. The
640 Polerovirus F box protein P0 targets ARGONAUTE1 to suppress RNA silencing. *Curr*
641 *Biol* **17**, 1615-21.

642 Bouvaine S, Boonham N, Douglas AE, 2011. Interactions between a luteovirus and the
643 GroEL chaperonin protein of the symbiotic bacterium *Buchnera aphidicola* of aphids. *J*
644 *Gen Virol* **92**, 1467-74.

645 Brennecke J, Aravin AA, Stark A*, et al.*, 2007. Discrete small RNA-generating loci as
646 master regulators of transposon activity in *Drosophila*. *Cell* **128**, 1089-103.

647 Castle SJ, Berger PH, 1993. Rates of growth and increase of *Myzus persicae* on virus-
648 infected potatoes according to type of virus-vector relationship. *Entomol Exp Appl* **69**,
649 51-60.

650 Castle SJ, Mowry TM, Berger PH, 1998. Differential settling by *Myzus persicae*
651 (Homoptera: Aphididae) on various virus infected host plants. *Ann of the Entomol Soc*
652 *Am* **91**, 661-7.

653 Charles H, Calevro F, Vinuelas J, Fayard JM, Rahbe Y, 2006. Codon usage bias and
654 tRNA over-expression in *Buchnera aphidicola* after aromatic amino acid nutritional
655 stress on its host Acyrthosiphon pisum. *Nucleic Acids Res* **34**, 4583-92.

656 Chen YR, Zheng Y, Liu B, Zhong S, Giovannoni J, Fei Z, 2012. A cost-effective method
657 for Illumina small RNA-Seq library preparation using T4 RNA ligase 1 adenylated
658 adapters. *Plant Methods* **8**, 41.

659 Cilia M, Tamborindeguy C, Fish T, Howe K, Thannhauser TW, Gray S, 2011. Genetics
660 coupled to quantitative intact proteomics links heritable aphid and endosymbiont protein
661 expression to circulative polerovirus transmission. *J Virol* **85**, 2148-66.

662 Clavijo G, Van Munster M, Monsion B, Bochet N, Brault V, 2016. Transcription of
663 densovirus endogenous sequences in the *Myzus persicae* genome. *J Gen Virol* **97**,
664 1000-9.

665 Day MF, 1955. The Mechanism of the transmission of *Potato leafroll virus* by aphids.
666 *Aust J Biol Sci* **8**, 498.

667 Deblasio SL, Johnson R, Mahoney J*, et al.*, 2015. Insights into the polerovirus-plant
668 interactome revealed by coimmunoprecipitation and mass spectrometry. *Mol Plant-*
669 *Microbe Interact* **28**, 467-81.

670 Ding SW, Voinnet O, 2007. Antiviral immunity directed by small RNAs. *Cell* **130**, 413-26.

671 Eskandari F, 1979. Evidence for lack of propagation of *Potato leafroll virus* in its aphid
672 vector, *Myzus persicae*. *Phytopathology* **69**, 45.

673 Feng Y, Krueger EN, Liu S, Dorman K, Bonning BC, Miller WA, 2017. Discovery of
674 known and novel viral genomes in soybean aphid by deep sequencing. *Phytobiomes* **1**,
675 36-45.

676 Francis F, Gerkens P, Harmel N, Mazzucchelli G, De Pauw E, Haubruge E, 2006.
677 Proteomics in *Myzus persicae*: effect of aphid host plant switch. *Insect Biochem Mol*
678 *Biol* **36**, 219-27.

679 Franco-Lara LF, Mcgeachy KD, Commandeur U, Martin RR, Mayo MA, Barker H, 1999.
680 Transformation of tobacco and potato with cDNA encoding the full-length genome of
681 *Potato leafroll virus*: evidence for a novel virus distribution and host effects on virus
682 multiplication. *J Gen Virol* **80 (Pt 11)**, 2813-22.

683 Gerardo NM, Altincicek B, Anselme C*, et al.*, 2010. Immunity and other defenses in pea
684 aphids, *Acyrthosiphon pisum*. *Genome Biol* **11**, R21.

685 Ghanim M, Brumin M, Popovski S, 2009. A simple, rapid and inexpensive method for
686 localization of *Tomato yellow leaf curl virus* and *Potato leafroll virus* in plant and insect
687 vectors. *J Virol Methods* **159**, 311-4.

688 Gildow F, D'arcy C, 1990. Cytopathology and experimental host range of
689 *Rhopalosiphum padi virus*, a small isometric RNA virus infecting cereal grain aphids. *J*
690 *Invert Pathol* **55**, 245-57.

691 Gildow FE, 1980. Increased production of alatae by aphids reared on oats infected with
692 *Barley yellow dwarf virus*. *Ann Entomol Soc Am* **73**, 343-7.

693 Gray S, Cilia M, Ghanim M, 2014. Circulative, "nonpropagative" virus transmission: an
694 orchestra of virus-, insect-, and plant-derived instruments. *Adv Virus Res* **89**, 141-99.

695 Guyomar C, Legeai F, Jousselin E, Mougel C, Lemaitre C, Simon JC, 2018. Multi-scale
696 characterization of symbiont diversity in the pea aphid complex through metagenomic
697 approaches. *Microbiome* **6**, 181.

698 Hansen AK, Moran NA, 2011. Aphid genome expression reveals host-symbiont
699 cooperation in the production of amino acids. *Proc Natl Acad Sci U S A* **108**, 2849-54.

700 Harrison BD, 1958. Studies on the behavior of *Potato leafroll* and other viruses in the
701 body of their aphid vector *Myzus persicae* (Sulz.). *Virol* **6**, 265-77.

702 Hodge S, Powell G, 2008. Do plant viruses facilitate their aphid vectors by inducing
703 symptoms that alter behavior and performance? *Environ Entomol* **37**, 1573-81.

704 Hodge S, Powell G, 2010. Conditional facilitation of an aphid vector, *Acyrthosiphon*
705 *pisum*, by the plant pathogen, *Pea enation mosaic virus*. *J Insect Sci* **10**, 155.

706 Hwang YT, Kalischuk M, Fusaro AF, Waterhouse PM, Kawchuk L, 2013. Small RNA
707 sequencing of *Potato leafroll virus*-infected plants reveals an additional subgenomic
708 RNA encoding a sequence-specific RNA-binding protein. *Virol* **438**, 61-9.

709 Ingwell LL, Eigenbrode SD, Bosque-Perez NA, 2012. Plant viruses alter insect behavior
710 to enhance their spread. *Sci Rep* **2**, 578.

711 Jaubert-Possamai S, Le Trionnaire G, Bonhomme J, Christophides GK, Rispe C, Tagu
712 D, 2007. Gene knockdown by RNAi in the pea aphid *Acyrthosiphon pisum*. *BMC*
713 *Biotechnol* **7**, 63.

714 Jaubert-Possamai S, Rispe C, Tanguy S*, et al.*, 2010. Expansion of the miRNA pathway
715 in the hemipteran insect *Acyrthosiphon pisum*. *Mol Biol Evol* **27**, 979-87.

716 Jiu M, Zhou XP, Tong L*, et al.*, 2007. Vector-virus mutualism accelerates population
717 increase of an invasive whitefly. *PLoS One* **2**, e182.

718 Karasev AV, Hu X, Brown CJ*, et al.*, 2011. Genetic diversity of the ordinary strain of
719 *Potato virus Y* (PVY) and origin of recombinant PVY strains. *Phytopathology* **101**, 778-
720 85.

721 Kennedy JS, Day MF, Eastop VF, Commonwealth Institute Of E, Commonwealth
722 Agricultural B, Executive C, 1962. *A conspectus of aphids as vectors of plant viruses*.
723 London: Commonwealth Institute of Entomology.

724 Kersch-Becker MF, Thaler JS, 2014. Virus strains differentially induce plant
725 susceptibility to aphid vectors and chewing herbivores. *Oecologia* **174**, 883-92.

726 Kliot A, Cilia M, Czosnek H, Ghanim M, 2014. Implication of the bacterial endosymbiont
727 Rickettsia spp. in interactions of the whitefly *Bemisia tabaci* with *Tomato yellow leaf curl*
728 *virus*. *J Virol* **88**, 5652-60.

729 Kramer M. Use of the posterior predictive distribution as a diagnostic tool for mized
730 models. In: Song W, ed. *Proceedings of the 26th Annuak Kansas State University*
731 *Conference on Applied Statistics in Agriculture*, *2014*. Manhattan, Kansas, 82-101.

732 Kutnjak D, Rupar M, Gutierrez-Aguirre I, Curk T, Kreuze JF, Ravnikar M, 2015. Deep
733 sequencing of virus-derived small interfering RNAs and RNA from viral particles shows
734 highly similar mutational landscapes of a plant virus population. *J Virol* **89**, 4760-9.

735 Langmead B, Trapnell C, Pop M, Salzberg SL, 2009. Ultrafast and memory-efficient
736 alignment of short DNA sequences to the human genome. *Genome Biol* **10**, R25.

737 Lee YS, Shibata Y, Malhotra A, Dutta A, 2009. A novel class of small RNAs: tRNA-
738 derived RNA fragments (tRFs). *Genes Dev* **23**, 2639-49.

739 Li F, Ding SW, 2006. Virus counterdefense: diverse strategies for evading the RNA-
740 silencing immunity. *Annu Rev Microbiol* **60**, 503-31.

741 Li H, Handsaker B, Wysoker A*, et al.*, 2009. The Sequence Alignment/Map format and
742 SAMtools. *Bioinformatics* **25**, 2078-9.

743 Li R, Gao S, Hernandez AG, Wechter WP, Fei Z, Ling KS, 2012. Deep sequencing of
744 small RNAs in tomato for virus and viroid identification and strain differentiation. *PLoS*
745 *One* **7**, e37127.

746 Luteijn MJ, Ketting RF, 2013. PIWI-interacting RNAs: from generation to
747 transgenerational epigenetics. *Nat Rev Genet* **14**, 523-34.

748 Mackinnon JP, 1961. Preference of aphids for excised leaves to whole plants. *Can J*
749 *Zool* **39**, 445-7.

750 Mauck K, Bosque-Pérez NA, Eigenbrode SD, De Moraes CM, Mescher MC, Fox C,
751 2012. Transmission mechanisms shape pathogen effects on host-vector interactions:
752 evidence from plant viruses. *Funct Ecol* **26**, 1162-75.

753 Mauck KE, De Moraes CM, Mescher MC, 2010. Deceptive chemical signals induced by
754 a plant virus attract insect vectors to inferior hosts. *Proc Natl Acad Sci U S A* **107**, 3600-
755 5.

756 Milne I, Stephen G, Bayer M*, et al.*, 2013. Using Tablet for visual exploration of second-
757 generation sequencing data. *Brief Bioinform* **14**, 193-202.

758 Mlotshwa S, Pruss GJ, Vance V, 2008. Small RNAs in viral infection and host defense.
759 *Trends Plant Sci* **13**, 375-82.

760 Moon JS, Domier LL, Mccoppin NK, D'arcy CJ, Jin H, 1998. Nucleotide sequence
761 analysis shows that *Rhopalosiphum padi virus* is a member of a novel group of insect-
762 infecting RNA viruses. *Virology* **243**, 54-65.

763 Mutti NS, Park Y, Reese JC, Reeck GR, 2006. RNAi knockdown of a salivary transcript
764 leading to lethality in the pea aphid, *Acyrthosiphon pisum*. *J Insect Sci (Ludhiana)* **6**, 1-
765 7.

766 Nault LR, 1997. Arthropod transmission of plant viruses: a new synthesis. *Ann Entomoll*
767 *Soc Ama* **90**, 521-41.

768 Ng JC, Falk BW, 2006. Virus-vector interactions mediating nonpersistent and
769 semipersistent transmission of plant viruses. *Annu Rev Phytopathol* **44**, 183-212.

770 Pickett JA, Wadhams LJ, Woodcock CM, Hardie J, 1992. The chemical ecology of
771 aphids. *Annual Rev Entomol* **37**, 67-90.

772 Pinheiro PV, Ghanim M, Alexander M*, et al.*, 2017. Host plants indirectly influence plant
773 virus transmission by altering gut cysteine protease activity of aphid vectors. *Mol Cell*
774 *Proteomics* **16**, S230-S43.

775 Pitino M, Coleman AD, Maffei ME, Ridout CJ, Hogenhout SA, 2011. Silencing of aphid
776 genes by dsRNA feeding from plants. *PLoS One* **6**, e25709.

777 Poliakov A, Russell CW, Ponnala L*, et al.*, 2011. Large-scale label-free quantitative
778 proteomics of the pea aphid-*Buchnera* symbiosis. *Mol Cell Proteomics* **10**, M110
779 007039.

780 Quast C, Pruesse E, Yilmaz P*, et al.*, 2013. The SILVA ribosomal RNA gene database
781 project: improved data processing and web-based tools. *Nucleic Acids Res* **41**, D590-6.

782 Ryabov EV, 2007. A novel virus isolated from the aphid *Brevicoryne brassicae* with
783 similarity to Hymenoptera picorna-like viruses. *J Gen Virol* **88**, 2590-5.

784 Ryabov EV, Keane G, Naish N, Evered C, Winstanley D, 2009. Densovirus induces
785 winged morphs in asexual clones of the rosy apple aphid, *Dysaphis plantaginea*. *Proc of*
786 *Natl Acad Sci, U S A* **106**, 8465-70.

787 Sabin LR, Zheng Q, Thekkat P*, et al.*, 2013. Dicer-2 processes diverse viral RNA
788 species. *PLoS One* **8**, e55458.

789 Sapountzis P, Duport G, Balmand S*, et al.*, 2014. New insight into the RNA interference
790 response against cathepsin-L gene in the pea aphid, *Acyrthosiphon pisum*: molting or
791 gut phenotypes specifically induced by injection or feeding treatments. *Insect Biochem*
792 *Mol Biol* **51**, 20-32.

793 Sattar S, Addo-Quaye C, Song Y, Anstead JA, Sunkar R, Thompson GA, 2012.
794 Expression of small RNA in *Aphis gossypii* and its potential role in the resistance
795 interaction with melon. *PLoS One* **7**, e48579.

796 Shen M, Xu Y, Jia R, Zhou X, Ye K, 2010. Size-independent and noncooperative
797 recognition of dsRNA by the *Rice stripe virus* RNA silencing suppressor NS3. *J Mol Biol*
798 **404**, 665-79.

799 Shigenobu S, Watanabe H, Hattori M, Sakaki Y, Ishikawa H, 2000. Genome sequence
800 of the endocellular bacterial symbiont of aphids *Buchnera* sp. APS. *Nature* **407**, 81-6.

801 Sobala A, Hutvagner G, 2011. Transfer RNA-derived fragments: origins, processing,
802 and functions. *Wiley Interdiscip Rev RNA* **2**, 853-62.

803 R Core Team, 2017. *R: A language and environment for statistical computing.* Vienna,
804 Austria: R Foundation for Statistical Computing.

805 Teixeira M, Sela N, Ng J*, et al.*, 2016. A novel virus from Macrosiphum euphorbiae with
806 similarities to members of the family Flaviviridae. *J Gen Virol* **97**, 1261-71.

807 Thompson DM, Parker R, 2009. Stressing out over tRNA cleavage. *Cell* **138**, 215-9.

808 Van Der Wilk F, Dullemans AM, Verbeek M, Van Den Heuvel, M. JFJ, 1997. Nucleotide
809 sequence and genomic organization of
810 *Acyrthosiphon pisum virus*. *Virol J* **238**, 353–62.

811 Van Munster M, Dullemans AM, Verbeek M*, et al.*, 2002. Sequence analysis and
812 genomic organization of *Aphid lethal paralysis virus*: a new member of the family
813 *Dicistroviridae*. *J Gen Virol* **83**, 3131-8.

814 Van Munster M, Dullemans AM, Verbeek M*, et al.*, 2003a. A new virus infecting *Myzus*
815 *persicae* has a genome organization similar to the species of the genus *Densovirus*. *J*
816 *Gen Virol* **84**, 165-72.

817 Van Munster M, Dullemans AM, Verbeek M*, et al.*, 2003b. Characterization of a new
818 densovirus infecting the green peach aphid *Myzus persicae*. *J Invert Pathol* **84**, 6-14.

819 Wang K, Hoeksema J, Liang C, 2018. piRNN: deep learning algorithm for piRNA
820 prediction. *PeerJ* **6**, e5429.

821 Weidemann H-L, 2009. Zur Vermehrung des Kartoffelblattrollvirus in der Blattlaus
822 Myzus persicae (Sulz.). *J Appl Entomol* **94**, 321-30.

823 Whyard S, Singh AD, Wong S, 2009. Ingested double-stranded RNAs can act as
824 species-specific insecticides. *Insect Biochem Mol Biol* **39**, 824-32.

825 Williamson C, Rybicki E, Kasdorf G, Von Wechmar M, 1988. Characterization of a new
826 picorna-like virus isolated from aphids. *J Gen Virol* **69**, 787-95.

827 Xu Y, Huang L, Fu S, Wu J, Zhou X, 2012. Population diversity of *Rice stripe virus*-
828 derived siRNAs in three different hosts and RNAi-based antiviral immunity in
829 *Laodelphgax striatellus*. *PLoS One* **7**, e46238.

830 Zheng Y, Gao S, Padmanabhan C*, et al.*, 2017. VirusDetect: An automated pipeline for
831 efficient virus discovery using deep sequencing of small RNAs. *Virol* **500**, 130-8.

833 **Table 1.** Number of reads obtained by Illumina deep sequencing of sRNAs generated in

834 aphid and plant samples.

Tissue	Treatment	Avg # of cleaned reads[a]	PLRV[b]	PVY[c]	MpDNV[d]	*B. aphidicola*	% *Buchnera* tRNAs[e]
Aphids	PLRV-infected potato[f]	5673826	64	79	2979	471394	10.8%
	Purified PLRV in 30% sucrose[c]	5966972	48	108	2845	723696	13.1%
	Mock-inoculated potato[f]	1898702	--	51	2196	633184	4.1%
	PVY-infected potato[f]	4909636	--	203	6830	1594164	7.3%
	30% sucrose	3270474	--	48	13340	1182707	12.5%
	30% sucrose[f]	1735400	--	14	6457	447774	14.8%
Potato leaves	PLRV-infected, 3 WPI[g]	1885542	21918	13	79	9187	2.9%
	PLRV-infected, 3 DPI[h]	1317272	3419	3	--	2203	8.4%
Turnip leaves	Turnips fed to aphids after feeding on PLRV-infected potato	1158558	108	33	37	12988	7.2%
	Turnips fed to aphids after feeding on purified PLRV	1873005	169	42	48	9283	4.2%

835

836 [a] The average number of cleaned reads reflects the average number of reads per

837 replicate after removal of adapter and rRNA sequences.

838 [b] *Potato leafroll virus* (PLRV)

839 [c] *Potato virus Y* (PVY)

840 [d] *Myzus persicae densovirus* (MpDNV)

841 [e] The percent of reads aligned to *B. aphidicola* that aligned to *B. aphidicola* tRNAs.

842 [f] After the initial treatment, all of these aphids were also moved to turnip for 3 days.

843 [g] WPI: weeks post inoculation.

844 [h] DPI: days post inoculation.

845 **FIGURE LEGENDS**

846 **Figure 1.** Length distribution of sRNA reads generated in aphids, which aligned to the
847 aphid genome. *M. persicae* aphids (~700 aphids/replicate, 3-4 replicates/treatment)
848 were given a 72 h AAP on PLRV-infected plants, purified PLRV in 30% sucrose, PVY-
849 infected potato plants, 30% sucrose, and mock-inoculated potato plants, followed by 72
850 h gut clearing on turnip plants for all treatments. Aphid sRNA was extracted,
851 sequenced, and analyzed as described in the methods. Values presented are the
852 percentage of reads of that size aligning to the *M. persicae* genome, averaged across
853 biological replicates. Error bars represent ± one standard error. Letters represent
854 significantly different size distributions ($p < 0.05$) using multinomial distribution
855 modeling.

856 **Figure 2.** sRNA mapping to the most abundant *B. aphidicola* aminoacyl-tRNAs in aphid
857 samples. *M. persicae* aphids (~700 aphids/replicate, 3-4 replicates/treatment) were
858 given a 72 h AAP on PLRV-infected plants, purified PLRV in 30% sucrose, PVY-
859 infected potato plants, 30% sucrose, and mock-inoculated potato plants, followed by 72
860 h gut clearing on turnip plants for all treatments. Aphid sRNA was extracted,
861 sequenced, and analyzed as described in the methods. Values presented as percent of
862 the total *Buchnera*-derived sRNA generated in aphids, averaged across biological
863 replicates. Shown are the abundance of sRNA reads mapping to the aminoacyl-tRNAs
864 asparagine (A), tyrosine (B), threonine (C), methionine (D), serine (E), leucine (F), and
865 glycine (G), in descending order of abundance. Error bars represent ± one standard
866 error. Letters represent significantly different treatments ($p < 0.05$).

867 **Figure 3.** Length distribution of sRNA reads generated in aphids, which aligned to the

genome of the aphid virus MpDNV. *M. persicae* aphids (~700 aphids/replicate, 3-4 replicates/treatment) were given a 72 h AAP on PLRV-infected plants, purified PLRV in 30% sucrose, PVY-infected potato plants, and mock-inoculated potato plants, followed by 72 h gut clearing on turnip plants for all treatments. Aphid sRNA was extracted, sequenced, and analyzed as described in the methods. Values presented are the percentage of reads of that size aligning to the MpDNV genome, averaged across biological replicates. Error bars represent ± one standard error. Letters represent significantly different size distributions ($p < 0.05$) using multinomial distribution modeling.

Figure 4. Quantification of *Myzus persicae densovirus* (MpDNV) in *Myzus persicae* aphids. Aphid DNA was extracted and MpDNV titer was quantified via droplet digital PCR. **A.** Aphids fed on PLRV-infected or PLRV-free hairy nightshade (*Solanum sarrachoides,* HNS) for three days (single aphids, 20 replicates per treatment). * indicates a p-value less than 0.05 (Kruskal-Wallis test, $p = 0.02$). **B.** Aphids fed on *Nicotiana benthamiana* plants transiently expressing a PLRV infectious clone (PLRV), the viral silencing suppressor P0 driven by the 35S promoter (P0), the same 35S construct expressing GFP (GFP), or non-infiltrated (healthy) plants (4-8 aphids per replicate, 10-12 replicates per treatment) for 1 day (top) or 3 days (bottom). Letters show significantly different treatments ($p < 0.05$) via the Kruskal-Wallis test. **C.** Winged and non-winged aphids (5 aphids per replicate/16 replicates per treatment) collected from the same uninfected *P. floridana* colony. *** indicates a p-value less than 0.001 (Mann-Whitney test, $p = 9.57 \times 10^{-5}$). Data are presented as copies of MpDNV found in 1 ng/μL of total aphid DNA. Boxes represent the interquartile range. The median is

891 designated as a dark black line. Whiskers reach to maximum and minimum values.
892 Circles are outliers.
893
894 **SUPPLEMENTAL MATERIAL**
895 **Figure S1.** Diagram of the experimental design of the sRNA-seq. Aphids (~700
896 aphids/replicate, 3-4 replicates/treatment) were given a three-day AAP on PLRV-
897 infected plants, purified PLRV in 30% sucrose, PVY-infected potato plants, 30%
898 sucrose, and mock-inoculated potato plants, followed by three days of gut clearing on
899 turnip plants for all treatments. After gut-clearing, aphids were collected. Turnip leaves
900 were collected from the plants used to clear the guts of aphids exposed to PLRV-
901 infected potato plants and purified PLRV in 30% sucrose. PLRV-infected potato tissue
902 was taken at the end of the three-day AAP after aphids were removed. These potato
903 plants were inoculated three weeks prior and were systemically infected. Not shown,
904 locally PLRV-infected potato tissue was also taken at 3 DPI. Aphid and plant tissue
905 were flash frozen for sRNA extraction, library prep, and sequencing as described in the
906 methods.
907 **Figure S2.** Size distribution of sRNA reads mapping to PLRV in potato samples. Values
908 presented are the number of reads of that size aligning to the PLRV genome, averaged
909 across biological replicates. Data are shown for 3 DPI and 3 WPI. Error bars represent
910 ± one standard error.
911 **Figure S3.** Alignment of sRNA reads from aphid samples to *Buchnera* tRNAs. sRNA
912 reads were aligned to the sequences of mature *B. aphidicola* tRNAs using Bowtie and
913 visualized with Tablet. Each mature tRNA shows a predominant distribution of sRNA

914 reads mapping either to the 5' or 3' ends, or to the center. Shown are the alignments for
915 asparagine, with the majority of reads mapping to the 5' end (A); arginine, with reads
916 mapping to the center of the mature tRNA (B); and leucine, with reads mapping to the
917 3'end (C). These tRNA were each chosen as representative of a pattern of read
918 distribution, with one of these three distribution patterns being observed for every *B.*
919 *aphidicola* aminoacyl-tRNA.

920 **Figure S4.** Fluorescence *In Situ* Hybridization (FISH) of MpDNV and PLRV in aphid
921 guts. Shown are guts of PLRV-viruliferous (A-H) and uninfected (I-L) *M. persicae*
922 aphids. Blue in all panels is DAPI staining of the nuclei. Red is staining of PLRV
923 sequence-specific FISH probe conjugated to Cy2. Green is staining of MpDNV specific-
924 sequence FISH probe conjugated to Cy3. Fg: foregut; mg: midgut, hg: hindgut.

925 **Figure S5.** Distribution of sRNA reads along the MpDNV genome in aphid samples. *M.*
926 *persicae* aphids (~700 aphids/replicate, 3-4 replicates/treatment) were given a 72 h AAP
927 on PLRV-infected plants, purified PLRV in 30% sucrose, PVY-infected potato plants,
928 and mock-inoculated potato plants, followed by 72 h gut clearing on turnip plants for all
929 treatments. Aphid sRNA was extracted, sequenced, and analyzed as described in the
930 methods. Values presented are the percentage of reads aligning to that position in the
931 MpDNV genome, averaged across biological replicates. (A) Genome organization of
932 MpDNV. Arrows represent the direction of transcription. Arrows above the axis
933 represent transcription from the sense strand, arrows below the axis represent
934 transcription from the antisense strand. The region amplified by primers to quantify
935 MpDNV is shown as a black box. (B) 21-22nt reads; (C) 34-38nt reads. Dark grey boxes
936 represent regions of DLS integration into the aphid genome. Beige shading represents

937 the non-structural protein (NS) ORFs on the sense strand. Lilac shading represents the
938 structural protein (SP) ORFs on the antisense strand. Reads above the axis map to the
939 sense strand. Reads below the axis map to the antisense strand. Graphs are to scale
940 with (A).

941 **Figure S6.** Silencing suppressor activity of the P0 protein as compared to WT PLRV. *N.*
942 *benthamiana* plants were co-infiltrated with *Agrobacterium tumefaciens* cultures
943 expressing GFP, dsGFP, and P0 or WT PLRV. GFP expression was photographed with
944 a Canon EOS Rebel T6s under UV light 4 DPI. Positive control: P19 protein from
945 *Tomato bushy stunt virus*; negative control: only GFP and dsGFP.

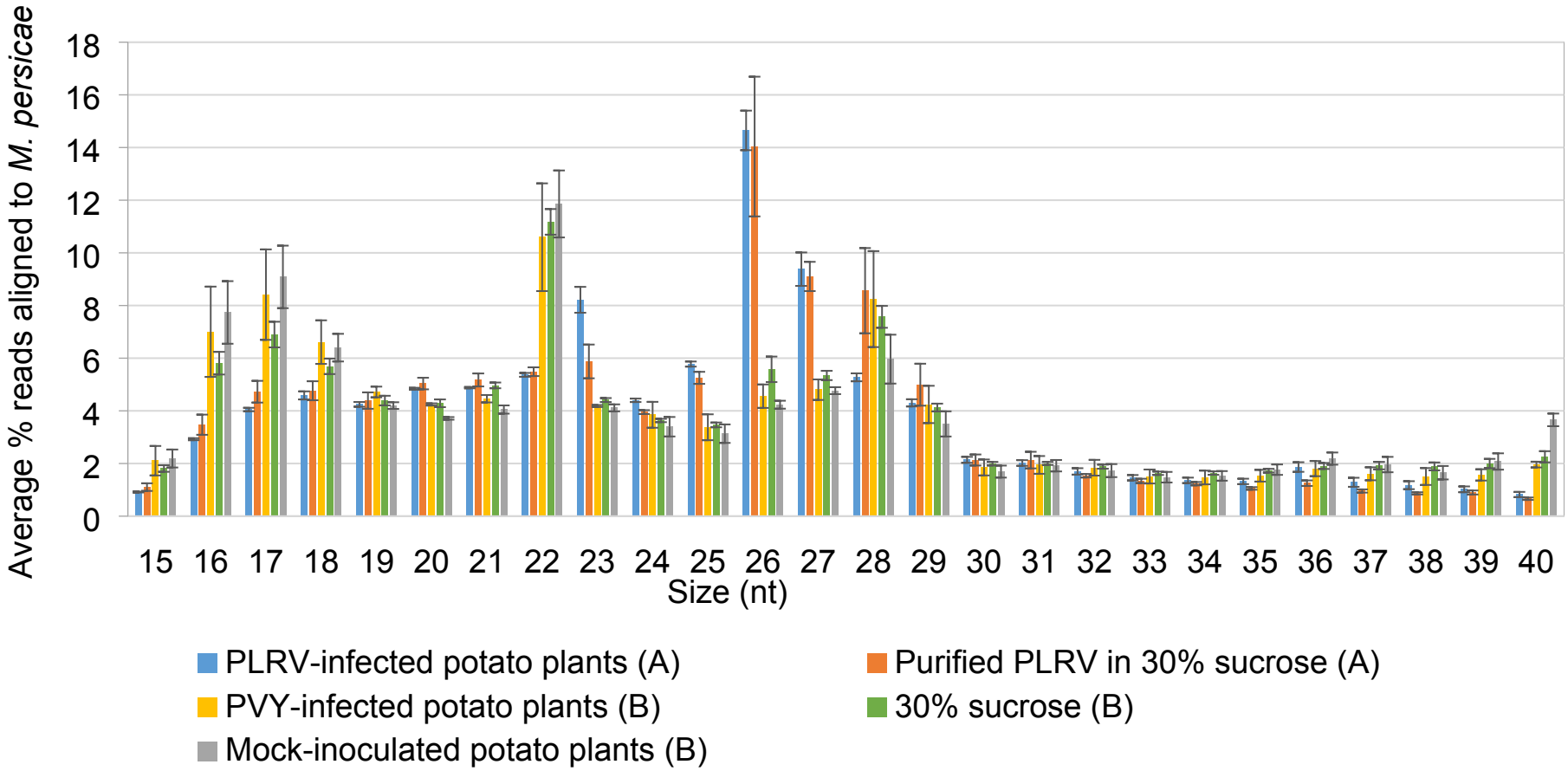

Figure 1. Length distribution of sRNA reads generated in aphids which aligned to the aphid genome. *M. persicae* aphids (~700 aphids/replicate, 3-4 replicates/treatment) were given a 72 h AAP on PLRV-infected plants, purified PLRV in 30% sucrose, PVY-infected potato plants, 30% sucrose, and mock-inoculated potato plants, followed by 72 h gut clearing on turnip plants for all treatments. Aphid sRNA was extracted, sequenced, and analyzed as described in the methods. Values presented are the percentage of reads of that size aligning to the *M. persicae* genome, averaged across biological replicates. Error bars represent ± one standard error. Letters represent significantly different size distributions ($p < 0.05$) using multinomial distribution modeling.

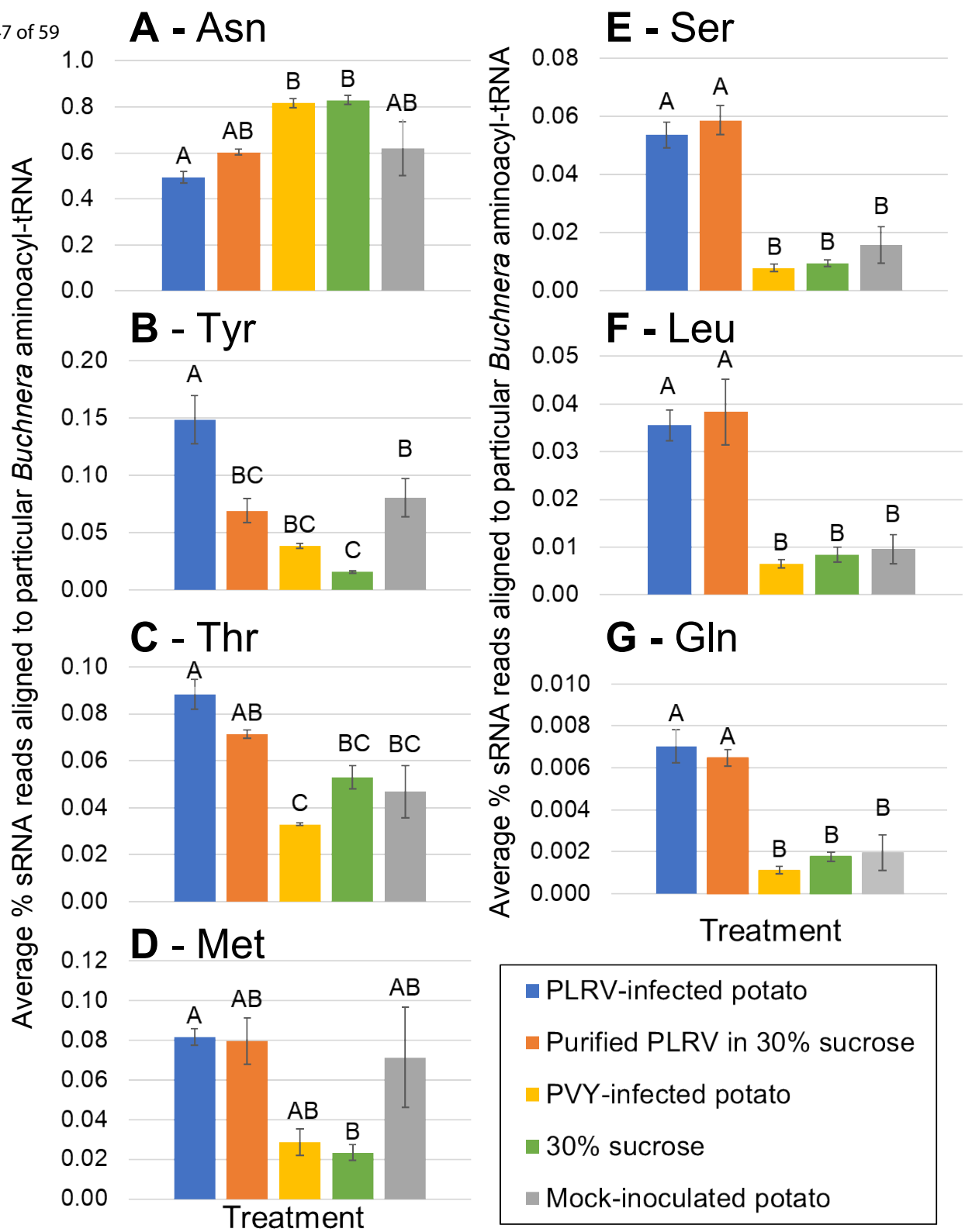

Figure 2. sRNA mapping to the most abundant *B. aphidicola* aminoacyl-tRNAs in aphid samples. *M. persicae* aphids (~700 aphids/replicate, 3-4 replicates/treatment) were given a 72 h AAP on PLRV-infected plants, purified PLRV in 30% sucrose, PVY-infected potato plants, 30% sucrose, and mock-inoculated potato plants, followed by 72 h gut clearing on turnip plants for all treatments. Aphid sRNA was extracted, sequenced, and analyzed as described in the methods. Values presented as percent of the total *Buchnera*-derived sRNA generated in aphids, averaged across biological replicates. Shown are the abundance of sRNA reads mapping to the aminoacyl-tRNAs asparagine (A), tyrosine (B), threonine (C), methionine (D), serine (E), leucine (F), and glycine (G), in descending order of abundance. Error bars represent ± one standard error. Letters represent significantly different treatments ($p < 0.05$).

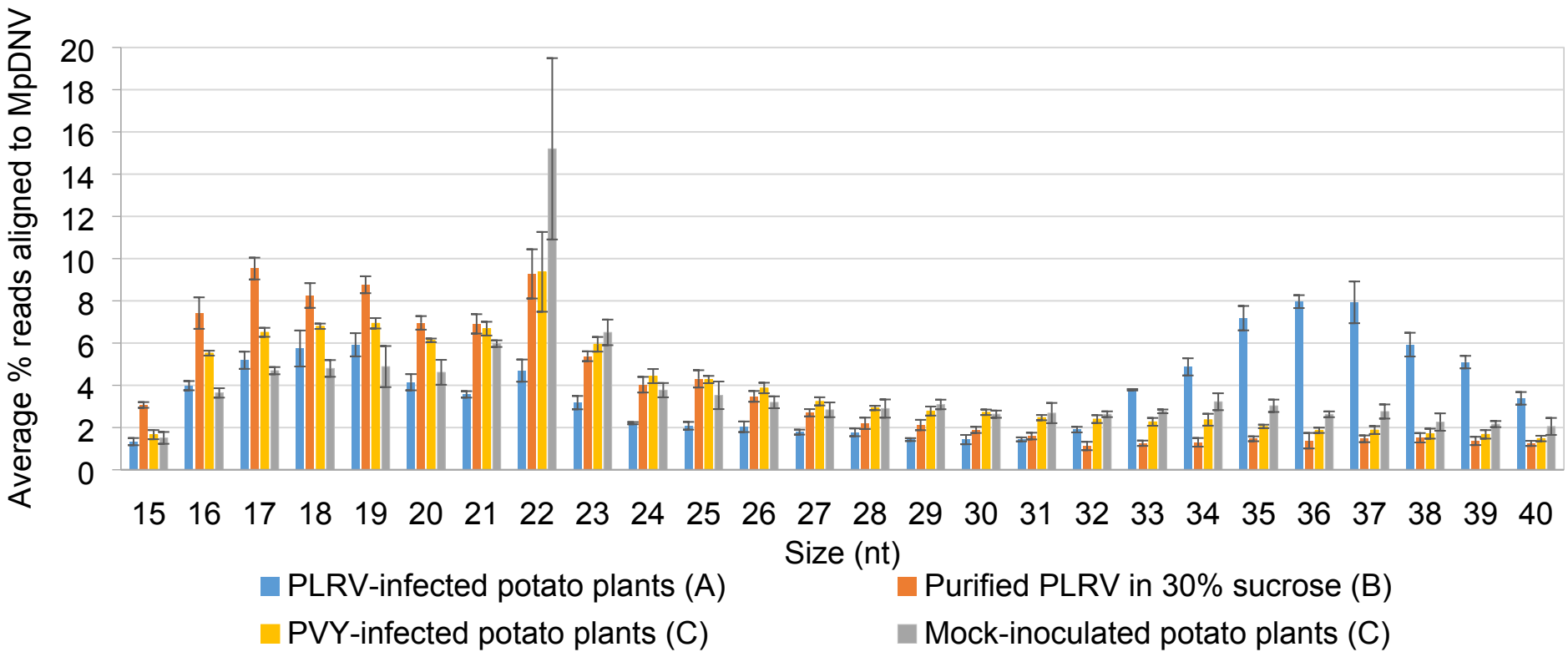

Figure 3. Length distribution of sRNA reads generated in aphids, which aligned to the genome of the aphid virus MpDNV. *M. persicae* aphids (~700 aphids/replicate, 3-4 replicates/treatment) were given a 72 h AAP on PLRV-infected plants, purified PLRV in 30% sucrose, PVY-infected potato plants, and mock-inoculated potato plants, followed by 72 h gut clearing on turnip plants for all treatments. Aphid sRNA was extracted, sequenced, and analyzed as described in the methods. Values presented are the percentage of reads of that size aligning to the MpDNV genome, averaged across biological replicates. Error bars represent ± one standard error. Letters represent significantly different size distributions ($p < 0.05$) using multinomial distribution modeling.

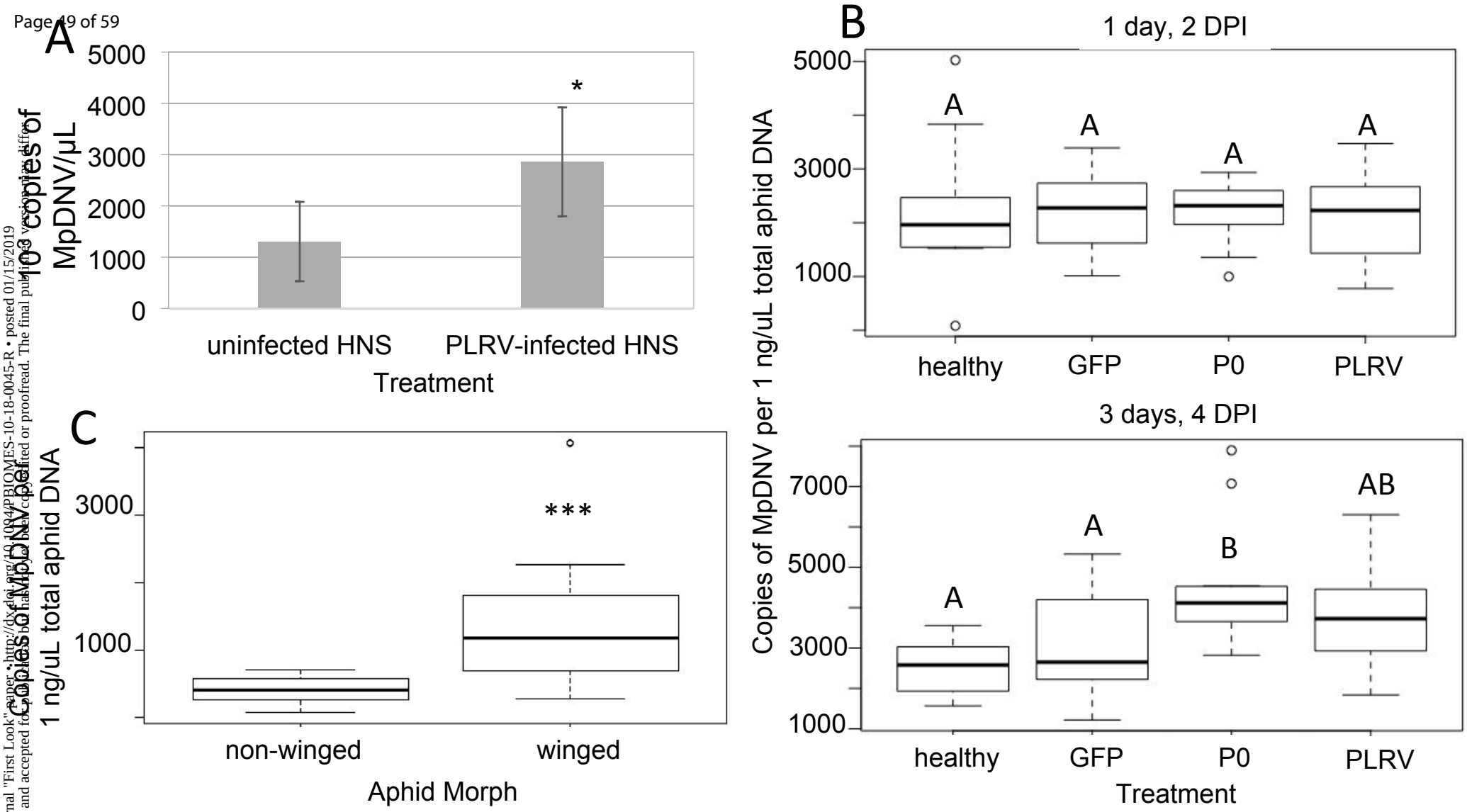

Figure 4. Quantification of *Myzus persicae densovirus* (MpDNV) in *Myzus persicae* aphids. Aphid DNA was extracted and MpDNV titer was quantified via droplet digital PCR. **A.** Aphids fed on PLRV-infected or PLRV-free hairy nightshade (*Solanum sarrachoides,* HNS) for three days (single aphids, 20 replicates per treatment). * indicates a p-value less than 0.05 (Kruskal-Wallis test, $p = 0.02$). **B.** Aphids fed on *Nicotiana benthamiana* plants transiently expressing a PLRV infectious clone (PLRV), the viral silencing suppressor P0 driven by the 35S promoter (P0), the same 35S construct expressing GFP (GFP), or non-infiltrated (healthy) plants (4-8 aphids per replicate, 10-12 replicates per treatment) for 1 day (top) or 3 days (bottom). Letters show significantly different treatments ($p < 0.05$) via the Kruskal-Wallis test. **C.** Winged and non-winged aphids (5 aphids per replicate/16 replicates per treatment) collected from the same uninfected *P. floridana* colony. *** indicates a p-value less than 0.001 (Mann-Whitney test, $p = 9.57 \times 10^{-5}$). Data are presented as copies of MpDNV found in 1 ng/µL of total aphid DNA. Boxes represent the interquartile range. The median is designated as a dark black line. Whiskers reach to maximum and minimum values. Circles are outliers.

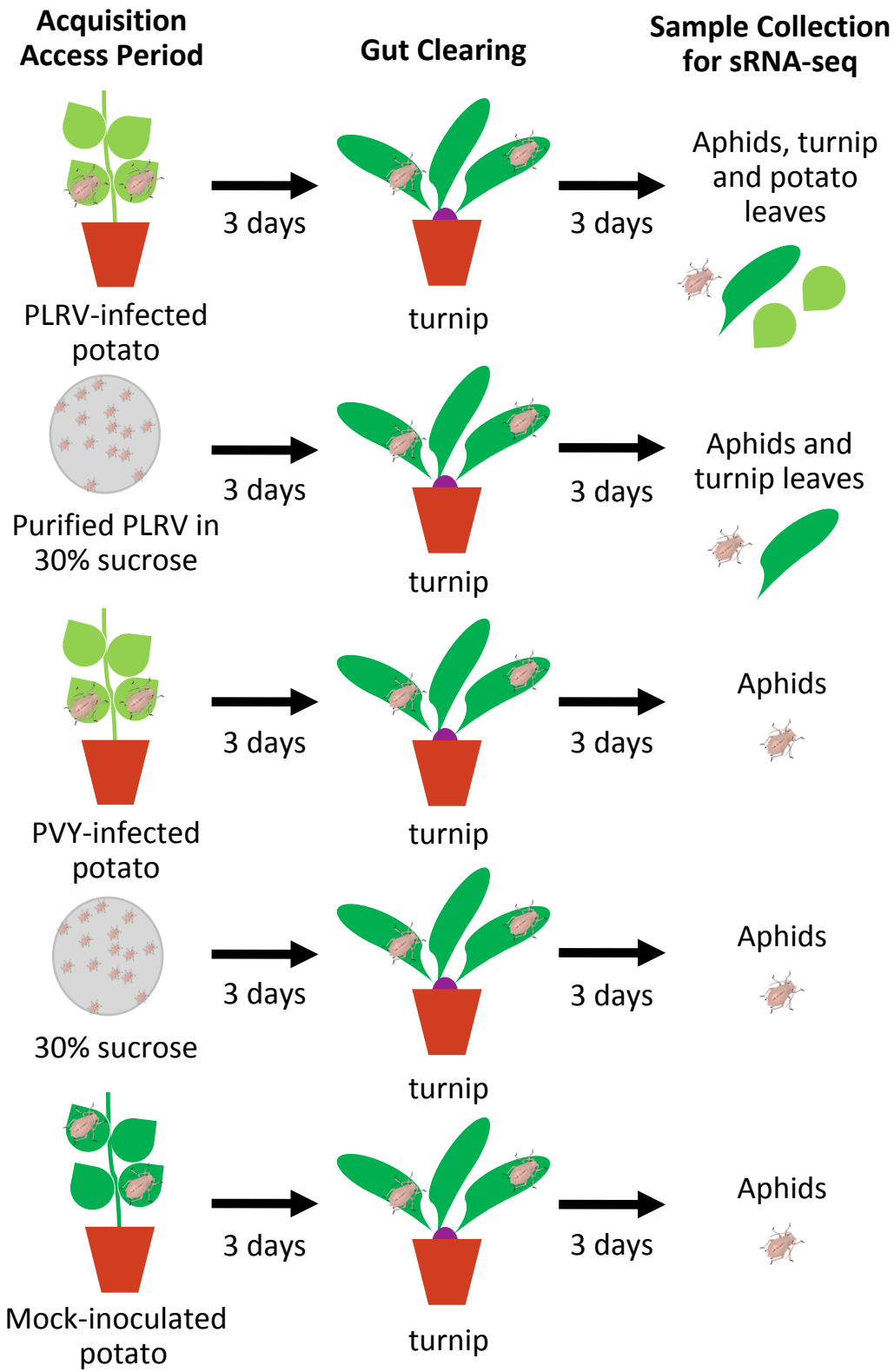

Figure S1. Diagram of the experimental design of the sRNA-seq. Aphids (~700 aphids/replicate, 3-4 replicates/treatment) were given a three-day AAP on PLRV-infected plants, purified PLRV in 30% sucrose, PVY-infected potato plants, 30% sucrose, and mock-inoculated potato plants, followed by three days of gut clearing on turnip plants for all treatments. After gut-clearing, aphids were collected. Turnip leaves were collected from the plants used to clear the guts of aphids exposed to PLRV-infected potato plants and purified PLRV in 30% sucrose. PLRV-infected potato tissue was taken at the end of the three-day AAP after aphids were removed. These potato plants were inoculated three weeks prior and were systemically infected. Not shown, locally PLRV-infected potato tissue was also taken at 3 DPI. Aphid and plant tissue were flash frozen for sRNA extraction, library prep, and sequencing as described in the methods.

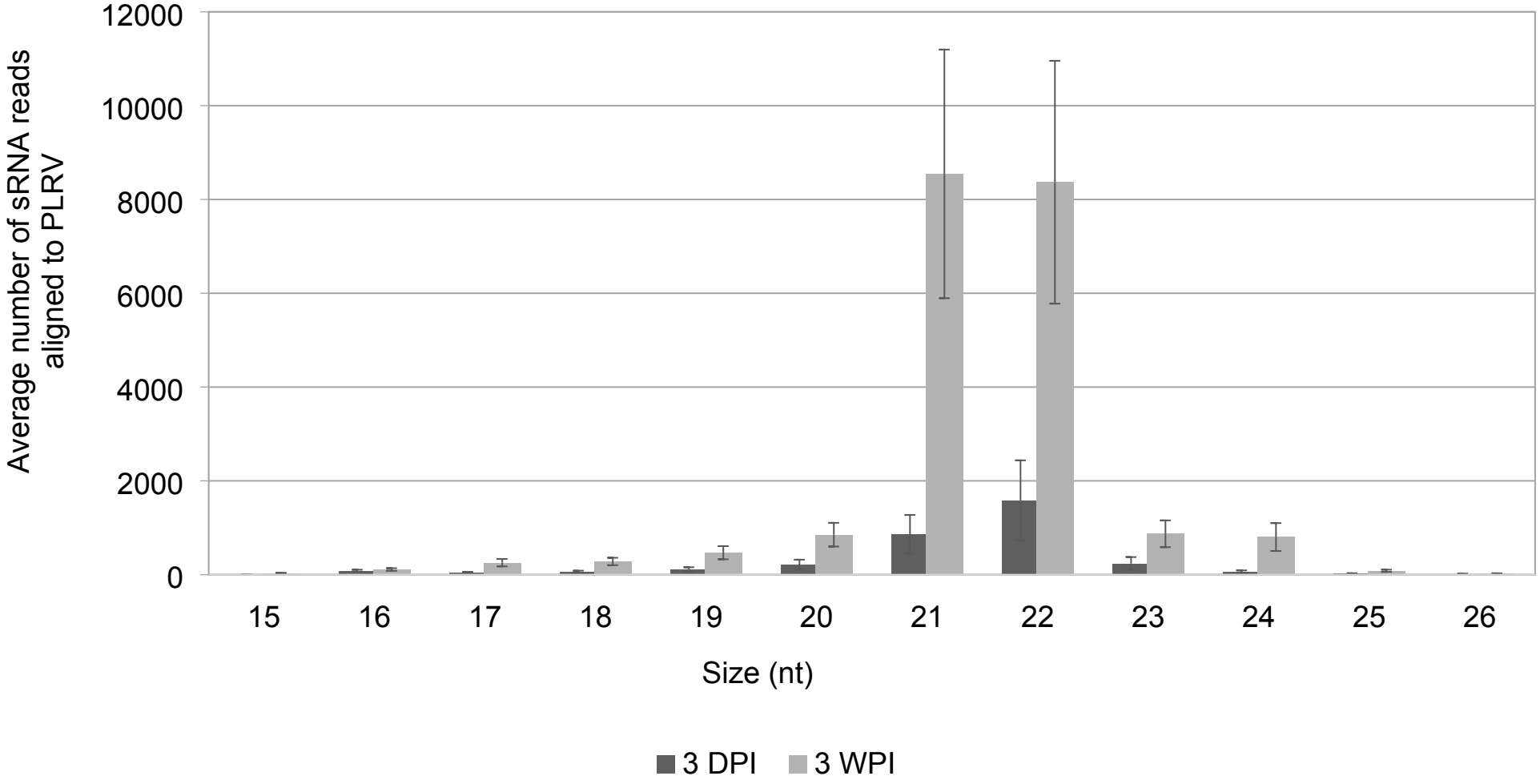

Figure S2. Size distribution of sRNA reads mapping to PLRV in potato samples. Values presented are the number of reads of that size aligning to the PLRV genome, averaged across biological replicates. Data are shown for 3 DPI and 3 WPI. Error bars represent ± one standard error.

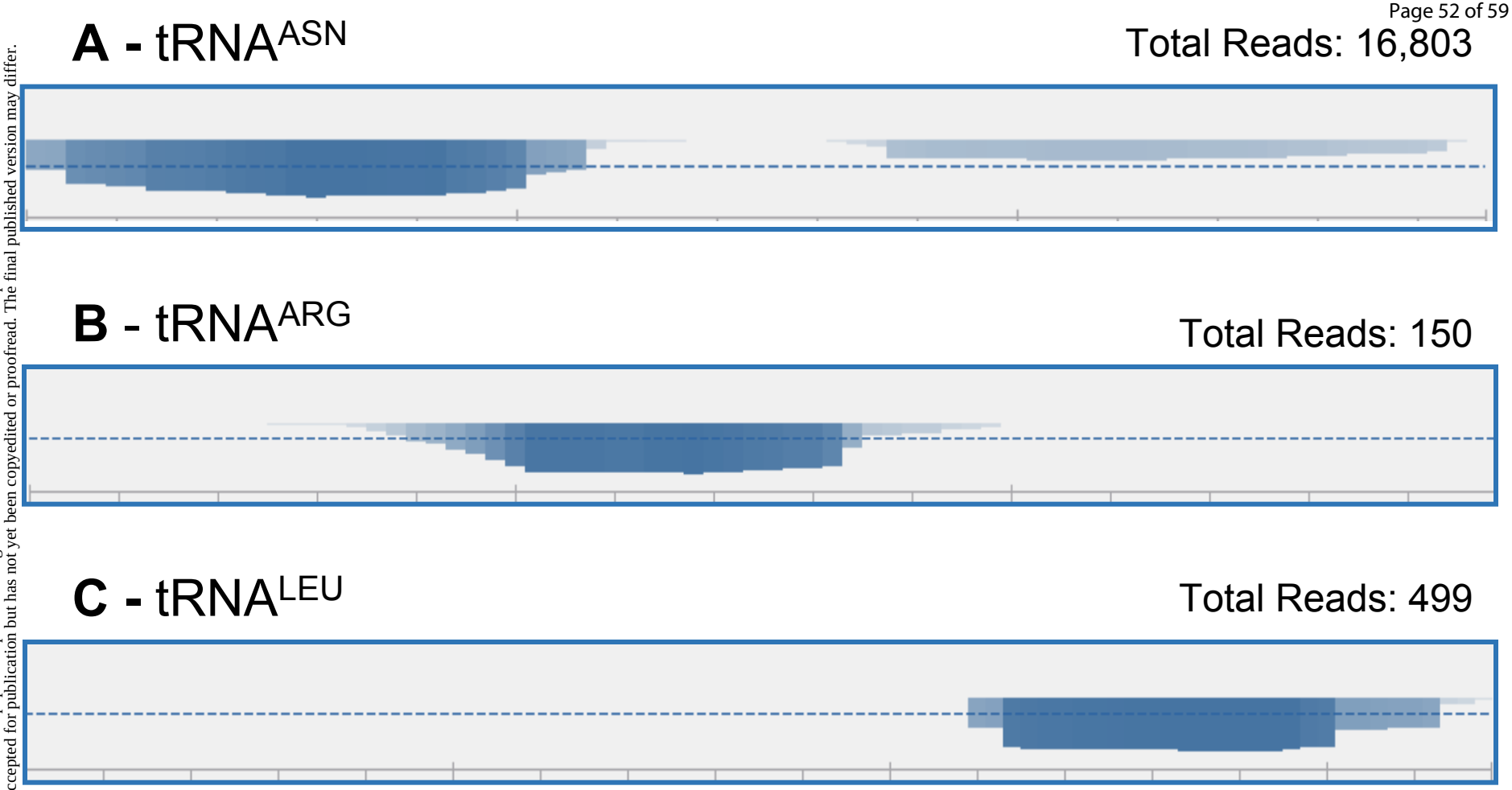

Figure S3. Alignment of sRNA reads from aphid samples to *Buchnera* tRNAs. sRNA reads were aligned to the sequences of mature *B. aphidicola* tRNAs using Bowtie and visualized with Tablet. Each mature tRNA shows a predominant distribution of sRNA reads mapping either to the 5' or 3' ends, or to the center. Shown are the alignments for asparagine, with the majority of reads mapping to the 5' end (A); arginine, with reads mapping to the center of the mature tRNA (B); and leucine, with reads mapping to the 3'end (C). These tRNA were each chosen as representative of a pattern of read distribution, with one of these three distribution patterns being observed for every *B. aphidicola* aminoacyl-tRNA.

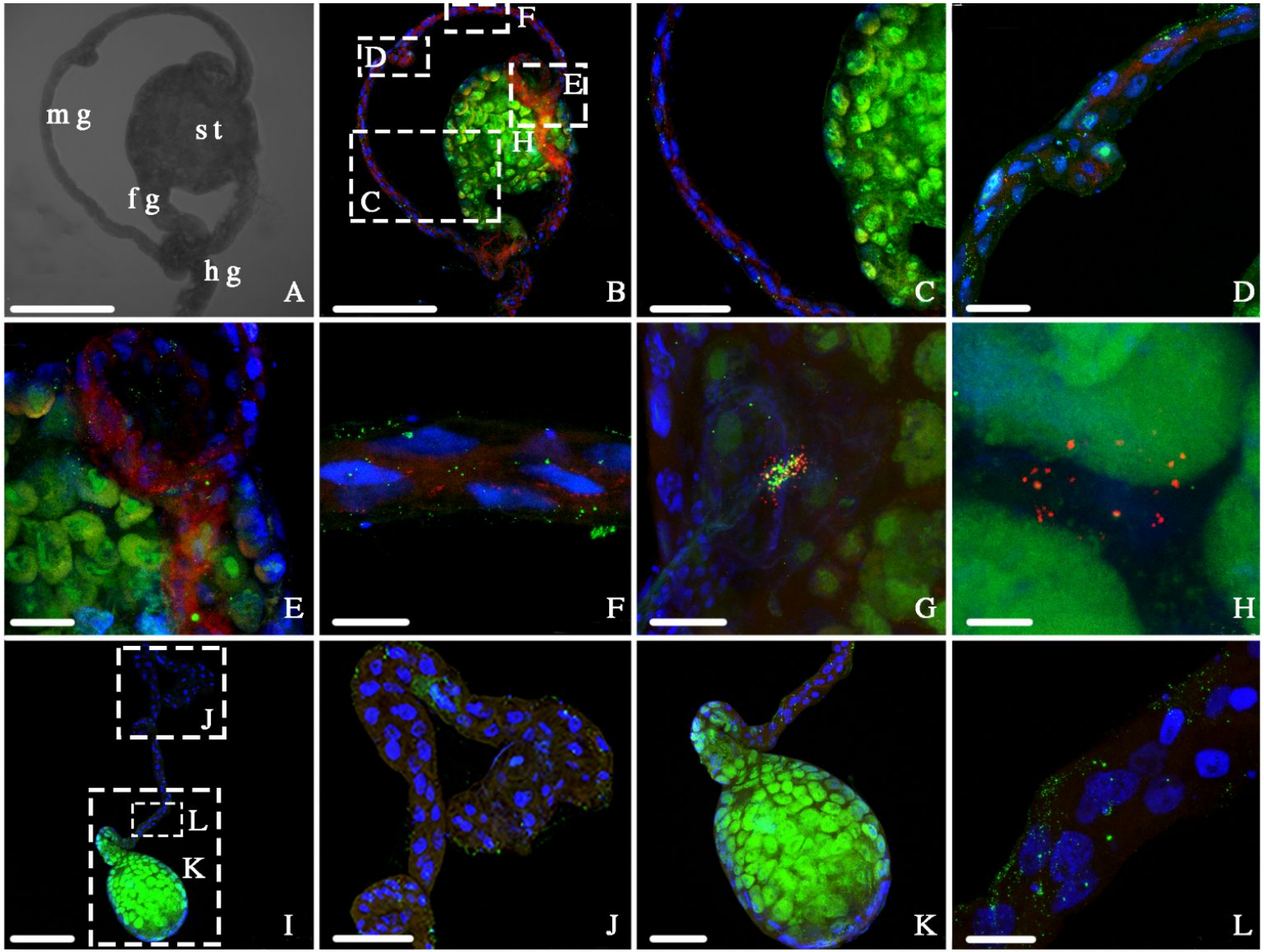

Figure S4. Fluorescence *In Situ* Hybridization (FISH) of MpDNV and PLRV in aphid guts. Shown are guts of PLRV-viruliferous (A-H) and uninfected (I-L) *M. persicae* aphids. Blue in all panels is DAPI staining of the nuclei. Red is staining of PLRV sequence-specific FISH probe conjugated to Cy2. Green is staining of MpDNV specific-sequence FISH probe conjugated to Cy3. Fg: foregut; mg: midgut, hg: hindgut.

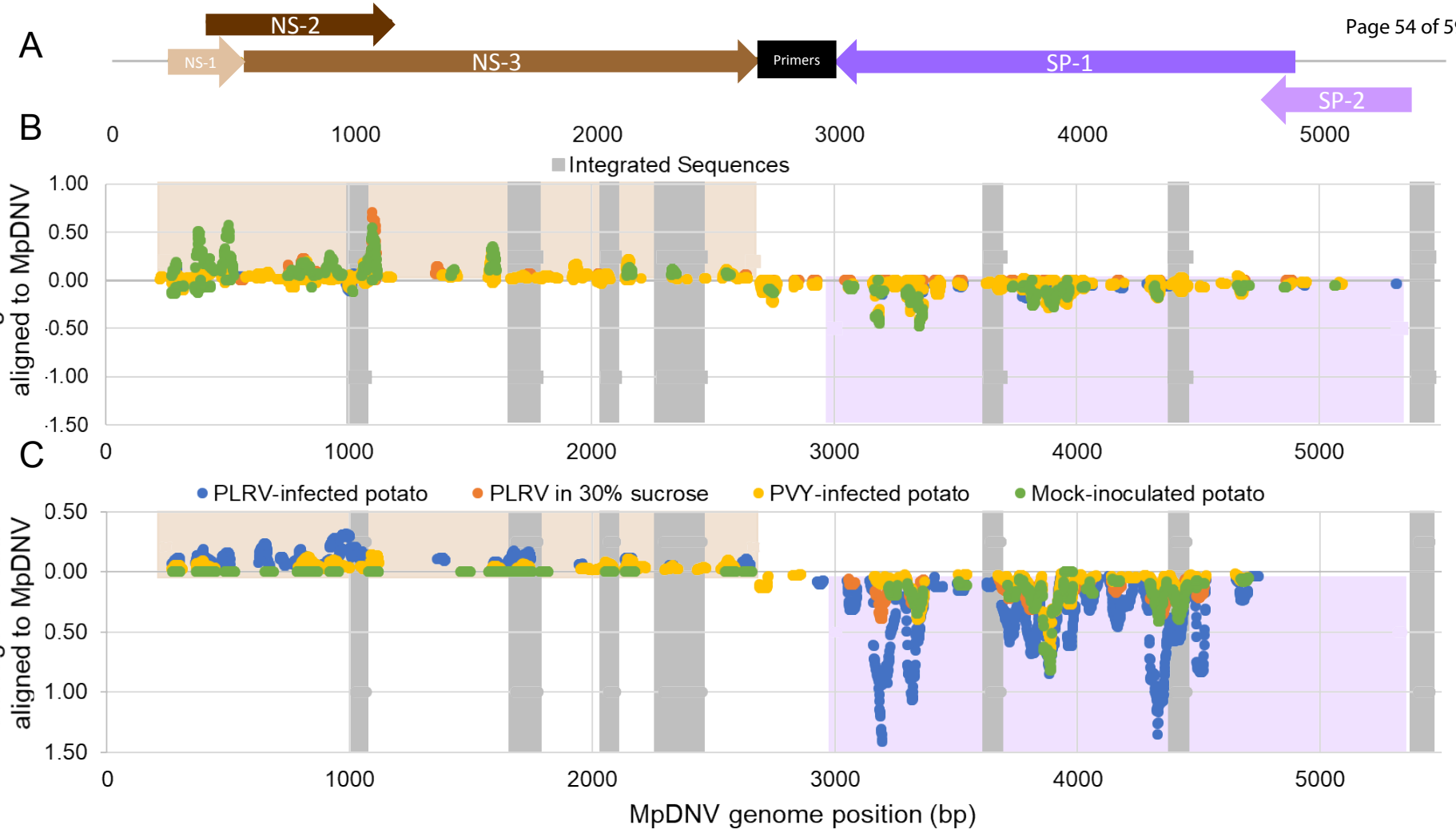

Figure S5. Distribution of sRNA reads along the MpDNV genome in aphid samples. *M. persicae* aphids (~700 aphids/replicate, 3-4 replicates/treatment) were given a 72 h AAP on PLRV-infected plants, purified PLRV in 30% sucrose, PVY-infected potato plants, and mock-inoculated potato plants, followed by 72 h gut clearing on turnip plants for all treatments. Aphid sRNA was extracted, sequenced, and analyzed as described in the methods. Values presented are the percentage of reads aligning to that position in the MpDNV genome, averaged across biological replicates. (A) Genome organization of MpDNV. Arrows represent the direction of transcription. Arrows above the axis represent transcription from the sense strand, arrows below the axis represent transcription from the antisense strand. The region amplified by primers to quantify MpDNV is shown as a black box. (B) 21-22nt reads; (C) 34-38nt reads. Dark grey boxes represent regions of DLS integration into the aphid genome. Beige shading represents the non-structural protein (NS) ORFs on the sense strand. Lilac shading represents the structural protein (SP) ORFs on the antisense strand. Reads above the axis map to the sense strand. Reads below the axis map to the antisense strand. Graphs are to scale with (A).

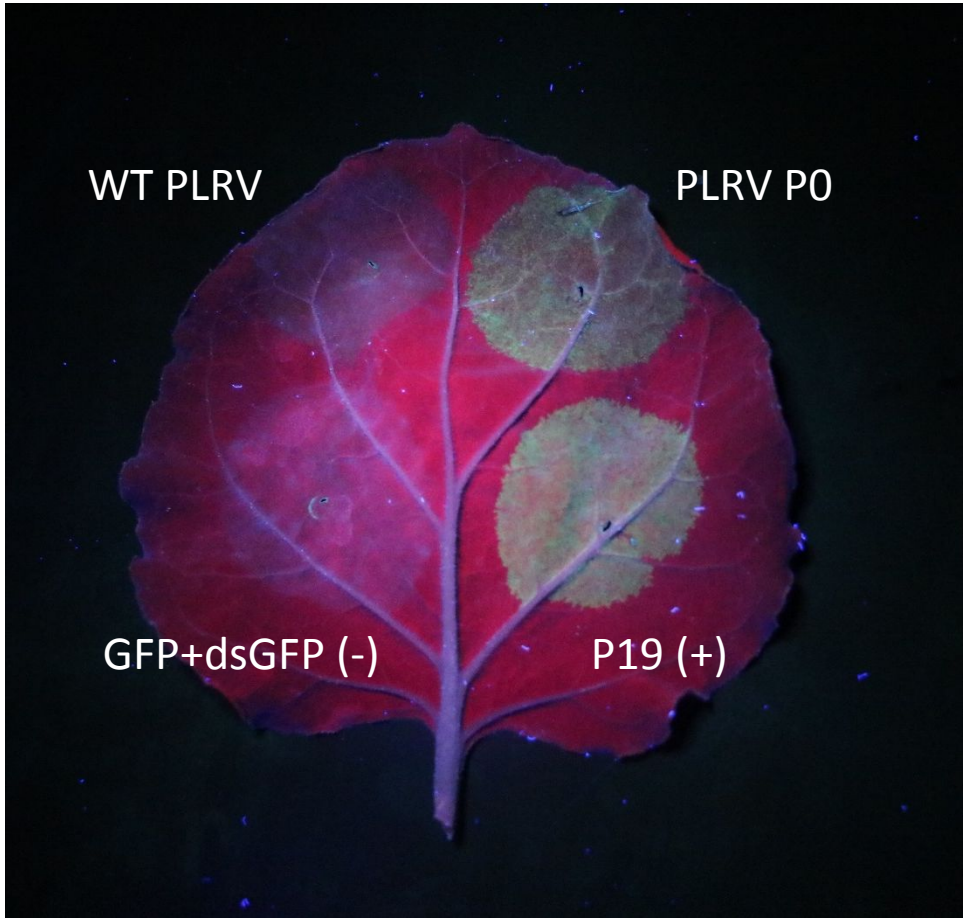

Figure S6. Silencing suppressor activity of the P0 protein as compared to WT PLRV. *N. benthamiana* plants were co-infiltrated with *Agrobacterium tumefaciens* cultures expressing GFP, dsGFP, and P0 or WT PLRV. GFP expression was photographed with a Canon EOS Rebel T6s under UV light 4 DPI. Positive control: P19 protein from *Tomato bushy stunt virus*; negative control: only GFP and dsGFP.

Table S1. The percent of 26 and 27nt reads mapping to the *M. persicae* genome predicted to be piRNA in aphids exposed to PLRV

Treatment	Replicate	Total # of 26-27 mers	# of predicted piRNA[a]	% piRNA	Avg % piRNA[b]
PLRV-infected potato	1	951,819	853,725	89.69	89.52 ± 0.90
	2	730,817	635,967	87.02	
	3	1,215,438	1,109,054	91.25	
	4	700,856	631,595	90.12	
Purified PLRV in 30% sucrose	1	1,374,308	1,283,418	93.39	91.83 ± 0.53
	2	441,516	401,765	91.00	
	3	796,779	729,266	91.53	
	4	793,825	725,719	91.42	

[a]piRNA prediction was performed using the piRNN deep learning algorithm using the *Drosophila melanogaster* model

[b]Average percent of reads predicted to be piRNA across biological replicates, ± one standard error

Table S2. *Buchnera* tRNA-derived small RNA in aphid and plant samples by tRNA gene, total number of reads, average of reads across replicates, and percentage of total *Buchnera* tRNA-derived sRNAs.

		Myzus fed on PLRV-infected potato			Myzus fed on purified PLRV in 30% sucrose			Myzus fed on mock-inoculated potato			Myzus fed on PVY-infected potato		
AA[a]	**Buchnera tRNA gene**	**Sum**	**Avg**	**% Total tRNA reads**	**Sum**	**Avg**	**% Total tRNA reads**	**Total**	**Avg Reads**	**% Total tRNA reads**	**Total**	**Avg Reads**	**% Total tRNA reads**
Ala	trna1-AlaGGC	0	0	0	1	0.25	0.0003	0	0	0	0	0	0
Arg	trna7-ArgACG	56	14	0.03	59	14.75	0.02	0	0	0	8	2.67	0.002
Arg	trna12-ArgCCG	33	8.25	0.02	41	10.25	0.01	1	0.33	0.001	33	11.00	0.01
Arg	trna17-ArgTCT	621	155.25	0.31	611	152.75	0.18	902	300.67	1.15	1932	644.00	0.55
Asn	trna15-AsnGTT	100243	25060.75	49.76	199617	49904.25	59.54	51989	17329.67	66.11	287227	95742.33	81.82
Asp	trna4-AspGTC	50	12.5	0.02	87	21.75	0.03	204	68.00	0.26	433	144.33	0.12
Cys	trna23-CysGCA	1827	456.75	0.91	2327	581.75	0.69	593	197.67	0.75	2378	792.67	0.68
Gln	trna21-GlnTTG	1522	380.5	0.76	2445	611.25	0.73	131	43.67	0.17	388	129.33	0.11
Glu	trna16-GluTTC	3	0.75	0.001	2	0.50	0.001	0	0	0	0	0	0
Gly	trna30-GlyTCC	322	80.5	0.16	135	33.75	0.04	19	6.33	0.02	53	17.67	0.02
Gly	trna10-GlyGCC	796	199	0.40	1446	361.50	0.43	1690	563.33	2.15	4738	1579.33	1.35
His	trna13-HisGTG	186	46.5	0.09	192	48.00	0.06	25	8.33	0.03	91	30.33	0.03
Leu	trna20-LeuTAG	109	27.25	0.05	110	27.50	0.03	19	6.33	0.02	66	22.00	0.02
Leu	trna22-LeuGAG	28	7	0.01	72	18.00	0.02	19	6.33	0.02	46	15.33	0.01
Leu	trna24-LeuTAA	7997	1999.25	3.97	12814	3203.50	3.82	656	218.67	0.83	2127	709.00	0.61
Lys	trna27-LysTTT	12116	3029	6.01	16690	4172.50	4.98	6572	2190.67	8.36	12221	4073.67	3.48
Met	trna9-MetCAT	9331	2332.75	4.63	15469	3867.25	4.61	3815	1271.67	4.85	7415	2471.67	2.11
Met	trna18-MetCAT	7436	1859	3.69	12997	3249.25	3.88	865	288.33	1.10	2037	679.00	0.58
Met	trna19-MetCAT	342	85.5	0.17	409	102.25	0.12	240	80.00	0.31	496	165.33	0.14
Phe	trna32-PheGAA	301	75.25	0.15	403	100.75	0.12	23	7.67	0.03	74	24.67	0.02
Pro	trna14-ProTGG	1929	482.25	0.96	3457	864.25	1.03	603	201.00	0.77	1468	489.33	0.42
Ser	trna5-SerTGA	624	156	0.31	626	156.50	0.19	230	76.67	0.29	810	270.00	0.23
Ser	trna6-SerGCT	9778	2444.5	4.85	17047	4261.75	5.08	145	48.33	0.18	528	176.00	0.15
Ser	trna8-SerGGA	1952	488	0.97	2609	652.25	0.78	714	238.00	0.91	1397	465.67	0.40
Thr	trna28-ThrTGT	17589	4397.25	8.73	24127	6031.75	7.20	3386	1128.67	4.31	11559	3853.00	3.29
Thr	trna31-ThrGGT	0	0	0	0	0	0	0	0	0	0	0	0
Trp	trna11-TrpCCA	8	2	0.004	6	1.50	0.002	2	0.67	0.003	27	9.00	0.01
Tyr	trna29-TyrGTA	26228	6557	13.02	21482	5370.50	6.41	5797	1932.33	7.37	13486	4495.33	3.84
Val	trna26-ValTAC	7	1.75	0.003	12	3.00	0.004	2	0.67	0.003	2	0.67	0.001

[a] AA: amino acid

[b] DPI: days post inoculation

[c] WPI: weeks post inoculation.

Myzus fed on 30% sucrose			Potato 3 DPI[b] with PLRV			Potato 3 WPI[c] with PLRV			Turnip fed to aphids after feeding on PLRV-infected potato			Turnip fed to aphids after feeding on purified PLRV		
Total	Avg Reads	% Total tRNA reads	Total	Avg Reads	% Total tRNA reads	Sum	Avg	% Total tRNA reads	Sum	Avg	% Total tRNA reads	Sum	Avg	% Total tRNA reads
0	0	0	0	0	0	0	0	0	0	0	0	0	0	0
15	5.00	0.003	0	0	0	0	0	0	0	0	0	0	0	0
55	18.33	0.01	0	0	0	1	0.33	0.12	0	0	0	0	0	0
1248	416.00	0.28	2	0.50	0.27	10	3.33	1.23	14	4.67	0.49	10	3.33	0.84
366751	122250.33	82.86	586	146.50	78.98	357	119.00	43.86	1444	481.33	50.95	565	188.33	47.44
1718	572.67	0.39	0	0	0	0	0	0	3	1.00	0.11	1	0.33	0.08
2608	869.33	0.59	1	0.25	0.13	6	2.00	0.74	20	6.67	0.71	7	2.33	0.59
771	257.00	0.17	1	0.25	0.13	6	2.00	0.74	49	16.33	1.73	21	7.00	1.76
0	0	0	0	0	0	0	0	0	0	0	0	0	0	0
107	35.67	0.02	0	0	0	1	0.33	0.12	4	1.33	0.14	8	2.67	0.67
6348	2116.00	1.43	8	2.00	1.08	10	3.33	1.23	31	10.33	1.09	21	7.00	1.76
98	32.67	0.02	1	0.25	0.13	2	0.67	0.25	2	0.67	0.07	2	0.67	0.17
36	12.00	0.01	0	0	0	0	0	0	2	0.67	0.07	1	0.33	0.08
105	35.00	0.02	0	0	0	0	0	0	0	0	0	0	0	0
3487	1162.33	0.79	5	1.25	0.67	20	6.67	2.46	97	32.33	3.42	34	11.33	2.85
11088	3696.00	2.51	34	8.50	4.58	97	32.33	11.92	337	112.33	11.89	154	51.33	12.93
8257	2752.33	1.87	16	4.00	2.16	35	11.67	4.30	110	36.67	3.88	41	13.67	3.44
1981	660.33	0.45	20	5.00	2.70	36	12.00	4.42	92	30.67	3.25	30	10.00	2.52
311	103.67	0.07	0	0	0	5	1.67	0.61	6	2.00	0.21	6	2.00	0.50
169	56.33	0.04	31	7.75	4.18	35	11.67	4.30	21	7.00	0.74	20	6.67	1.68
2837	945.67	0.64	2	0.50	0.27	12	4.00	1.47	32	10.67	1.13	9	3.00	0.76
756	252.00	0.17	3	0.75	0.40	4	1.33	0.49	10	3.33	0.35	2	0.67	0.17
1767	589.00	0.40	0	0	0	33	11.00	4.05	87	29.00	3.07	74	24.67	6.21
1702	567.33	0.38	1	0.25	0.13	14	4.67	1.72	27	9.00	0.95	6	2.00	0.50
23170	7723.33	5.24	18	4.50	2.43	78	26.00	9.58	310	103.33	10.94	108	36.00	9.07
0	0	0	0	0	0	1	0.33	0.12	0	0	0	0	0	0
5	1.67	0.001	0	0	0	0	0	0	1	0.33	0.04	0	0	0
7202	2400.67	1.63	13	3.25	1.75	51	17.00	6.27	135	45.00	4.76	69	23.00	5.79
1	0.33	0.0002	0	0	0	0	0	0	0	0	0	2	0.67	0.17

Table S3. The regions of the *M. persicae* genome with high similarity when aligned to the MpDNV genome.

Scaffold # in *M. persicae* genome[a]	Score	e-value[b]	Position in MpDNV genome[c]	Position in *M. persicae* genome[a]	Length	% Identity
445	188	3.00E-45	1682-1776	43297-43203	95	100
400	84	1.00E-13	1027-1068	64852-64811	42	100
104	82	5.00E-13	3642-3686	540059-540103	41	97
538	72	4.00E-10	5404-5455	62318-62267	36	92
1839	70	2.00E-09	2295-2453	6854-7012	158	80
1839	62	4.00E-07	4402-4452	8660-8710	51	90
139	64	1.00E-07	2066-2097	212010-211979	32	100
139	56	3.00E-05	2058-2085	211954-211927	28	100
794	58	7.00E-06	2292-2344	16432-16484	53	88
794	54	1.00E-04	4402-4452	18326-18376	51	88

[a] *Myzus persicae* genome, clone G006, aphidbase.org

[b] The dotted line represents the e-value cut-off of 10^{-5}

[c] *Myzus persicae Densovirus,* GenBank Acc. No AY148187